EVALUATION OF EL836
EXPLOSIVE STIMULATION
OF DEVONIAN GAS SHALE

SCIENCE
APPLICATIONS
INCORPORATED

EVALUATION OF EL836
EXPLOSIVE STIMULATION
OF DEVONIAN GAS SHALE

Sub-task Technical Report
EGSP Support Contract Task 21
Contract No. DE-AT21-78MC08216

Prepared by

Timothy G. Barbour

Science Applications, Incorporated
206 West Magnolia Street
Fort Collins, Colorado 80521

September 1980

Prepared for

Department of Energy
Morgantown Energy Technology Center
Morgantown, West Virginia 26505

EXECUTIVE SUMMARY

As a part of Science Applications' involvement in the Eastern Gas Shales Project, a research program is being conducted to evaluate unconventional wellbore stimulation technologies. Included in this effort is the development of numerical models to describe and predict laboratory experiment and field demonstration results. The numerical model development is also being used in parameter sensitivity analyses to determine the importance of various aspects of the dynamic wellbore loading phenomenology.

This report presents an evaluation of EL836, an explosive developed at E.I. duPont de Nemours and Company Laboratories, in stimulating gas shale. EL836 is a water gel type explosive with a high aluminum content. Typically, this explosive completely fills the borehole. Its characteristics include very high energy, high heat of explosion and relatively low explosion pressure. It also has the benefits of maximum gas evolution and very little water content in the detonation products. The composition, loading conditions and characteristics of EL836 are quite different from those of other unconventional stimulation treatments which generally use a propellant charge by itself or in conjunction with conventional explosives and decoupling fluids.

The computational evaluation of EL836 involved four one-dimensional cylindrical geometry calculations to assess the influence of two equation-of-state descriptions of EL836, the effect of rock yielding and the effect of internal crack pressurization.

Results of a computational evaluation of the EL836 explosive in stimulating Devonian gas shale suggest the following:

- Extensive plastic yielding will occur in a region immediate to the borehole. For typical gas shale, this region extends to about three borehole radii.

- Extensive tensile fracture will occur in a region that begins at the outer boundary of plastic deformation and terminates at more than 100 borehole radii (approximately 10 meters).

- Without a mechanism of near-wellbore fracture, such as crushing or pre-cracking during drilling or intentional borehole grooving, the plastic flow that occurs adjacent to the wellbore causes stress redistributions which prohibit early-time (less than a millisecond) tensile fracture immediate to the wellbore and thus prohibits gas penetration from the wellbore into the crack system.

- The barrier that the near-wellbore plastic zone presents to gas flow from the wellbore is reduced in radial dimension as time increases. It would thus be expected that at late times in the EL836 stimulation treatment breakthrough would be achieved, enabling gas penetration into the crack system.

- Natural fractures in the wellbore wall or cataclysmic deformation and fracture adjacent to the wellbore, as a result of the explosive detonation, will likely assist in breaking down the barrier to gas flow, and thus enable early-time gas penetration.

- Very significant enhancement is achieved in the EL836 stimulation treatment when gases penetrate the stress-wave induced radial cracks. Crack opening is increased by an order-of-magnitude and crack extension is improved.

- Only minor differences were observed in the EL836 stimulation effects when comparison is made between two different explosive equations-of-state.

PREFACE

The Eastern Gas Shales Project (EGSP) of the Department of Energy (DOE) has the goal of examining marginal gas resources and to determine what methods would be required to extract vast amounts of natural gas trapped in eastern Devonian shales. As part of this project the Morgantown Energy Technology Center (METC) is conducting a research program to evaluate stimulation technologies in these relatively impermeable gas shales. One aspect of this program is concerned with numerical model development which would be used in assessing the suitability of various stimulation treatments. Part of this study is being conducted by Science Applications, Incorporated (SAI) under contract to METC. This report presents the results of a computational evaluation of the EL836 explosive, developed by duPont Laboratories, in stimulating the Devonian gas shale. It additionally describes a fluid flow model to account for wellbore fluid penetration into induced fractures.

CONTENTS

TABLES

LIST OF FIGURES

1. INTRODUCTION

Dynamic stimulation techniques which create multiple fractures in a wellbore have been the focus of several recent laboratory, field and computational investigations (1-4). These efforts have been directed towards an understanding of the basic phenomenology of explosive wellbore stimulation and the development of numerical codes to model the observed response. Primary conclusions of these studies substantiate what has been postulated for sometime. Namely, that conventional high-strength explosive detonation in a wellbore has the detrimental effects of wellbore crushing and rock yielding which impedes multiple fracture growth from the wellbore. The wellbore damage that results is also believed to limit penetration of the high-pressure gaseous detonation reaction products into possible stress-wave induced fractures outside the damage zone. An awareness of these effects has resulted in the development of numerous unconventional stimulation techniques which attempt to induce multiple fracture growth from a wellbore without the detrimental effects of borehole crushing, rock yielding, stress cage development, etc.

Aside from basic configuration changes, such as modification of the charge geometry or location in the wellbore relative to the pay formation, unconventional stimulation techniques are primarily directed towards optimization of the wellbore loading pulse to initiate multiple fractures without undue wellbore damage and with penetration of wellbore fluids into initiated cracks to open and extend the fractures for relatively long distances from the borehole. Tailoring the pulse, that the wellbore wall experiences, has been attempted in a number of ways. One method uses a small diameter conventional explosive charge centralized in a water-filled borehole (5). The intent is to decouple the sharp, high-amplitude explosive pulse from the rock wall by means of a water buffer. Peak stresses at the wellbore wall are intended to be below the rock yield stress. The total explosive energy, however, is limited by the small charge size. To extend the pressure pulse duration, this method has been used in an augmented mode where a propellant is

burned to drive the water into the explosive-initiated multiple cracks. Another method uses a small-diameter pressure-insensitive propellant charge that is centralized in a water-filled borehold (6). The device is designed to push water into initiated cracks ahead of the gas generated as reaction products of the burning propellant. The peak pressures of this device are well below typical rock yield stress and the pulse rise-time is sufficient to initiate multiple fractures. Still another method uses a full wellbore of propellant and the gas reaction products are themselves pushed into the initiated cracks (7).

Quite different in concept, from those mentioned, is the wellbore stimulation technique being developed by duPont Laboratories. The goal is the same; initiate multiple fractures with a sufficiently high loading rate and extend them by internal pressurization. The primary difference is the amount of explosive used and the composition, volume, energy, and pressure of the gas released. DuPont's EL836 explosive has the following characteristics (8):

- Safer than dynamite.
- More energy per unit mass or volume of explosive than dynamite or nitroglycerine and can be loaded to fill all the available borehole volume.
- Detonation products per unit mass and per unit volume of explosive contain more moles of gas and a smaller mole fraction of steam than nitroglycerine or dynamite.
- For conventionally loaded charges (EL836 completely filling the borehole volume vs 80% High Velocity Gelatin dynamite and 30% void volume) the calculated isentropic expansion work and expansion volume down to 0.0276GPA (4000 psi) for EL836 are, respectively, 2.40 and 1.97 times those of the dynamite. To the extent that steam condenses, these factors will be larger.
- The explosion pressure for EL836 completely filling the borehole is, respectively, about 1.41 and 2.76 times those of nitroglycerine loaded with 30% void space and the dynamite loaded with 30% void space.

Its use in well stimulation is in a fully-coupled mode (i.e., explosive completely fills the wellbore) intended to provide maximum energy availability. A full scale shot of 60,000 pounds of EL836 in a hole reamed to 15 inches in diameter has been conducted (8). DuPont is presently engaged in a 13-well test series in Devonian shale in Putnam County, WV at depths of 4,000-5,000 ft. Charge lengths of about 600 ft. will be used to compare five wells loaded with cartridged dynamite, (5 inch dia, 6,000 lb), five 6.25 inch open holes with EL836 (12,000 lb) and three holes underreamed to 12 inch diameter with EL836 (about 40,000 lb).

As of this writing five have been shot with EL836, one of which was underreamed to contain a 37,500 lb. charge. The following description of EL836, prepared by D.L. Coursen of duPont (9), presents details of its behavior and use in wellbore stimulation:

"EL836 is an explosive of the water gel type.

It contains monomethylamine nitrate and high content of aluminum formulated so as to result in complete reaction of the aluminum, as inferred from bubble pulse energies in underwater explosion tests. A substantial amount of its high heat of explosion (7.18 MJ/kg) results from the reaction

$$2\ AL + 3\ H_2O \rightarrow Al_2O_3 + 3\ H_2 + 8.86\ MJ/kg.$$

Its calculated CJ pressure of about 115 kbar and calculated explosion pressure of about 54 kbar are relatively low for an explosive of such high energy content, a desirable characteristic for applications such as well stimulation where excessive crushing of rock in the wall of the borehole is to be avoided. At the same time, the high temperature of its detonation products results in a relatively gradual fall in calculated pressure along its isentrope, which would be expected to result in relatively long extension of any gas-pressured radial fractures. Little steam remains after reaction with the aluminum, so little water can condense in gas-pressured fractures and also minimize deleterious effects of condensed water in them, particularly in water-sensitive rocks.

EL836 will detonate under high hydrostatic heads generated by well fluids or the explosive column itself. Its rheology can be varied from that of a pituitous fluid to that of a cohesive gel as required to conform with conditions in the well and the loading method used. Therefore, unlike the charges used in conventional shooting with dynamite or nitroglycerine where an annulus must be left between the rigid package and the hole and the charge diameter must be less than the minimum hole diameter, a charge of EL836 can fill all the available volume in the section of hole to be stimulated, even in underreamed holes. The loading density of a charge in place can range from 1.25 to 1.55, depending on the loading method used, the size of the hole, and the height of the column.

EL836 is marginally cap sensitive and has the safety characteristics typical of water gel compositions. Also it has shown satisfactory thermal stability in the presence of Tesorro crude oil at downhole temperatures typical of the Austin Chalk."

The objective of the effort by Science Applications is to perform a computational investigation of the EL836 in stimulating the Devonian gas shale. The evaluation uses the STEALTH (10) stress-wave propagation code with the CAVS (11) fracture model to numerically simulate the detonation

of EL836 in a wellbore in shale and the ensuing formation deformation and fracture. Included in the calculations are the effects of rock yielding, stress-wave-induced and internal crack pressurization-assisted tensile fracture, crack propping and gas penetration into the induced fractures. Four one-dimensional cylindrical geometry calculations were performed to assess the influence of two different equations-of-state descriptions of EL836 and the degree of rock yielding and the influence of gas pressurization. Section 2 describes the equation-of-state for EL836. Section 3 summarizes the Devonian gas shale material description used in the calculations. Calculational results are presented in Section 4, including the CAVS computed fracture distributions. Section 5 summarizes the results for the evaluation including the effects on stimulation of rock yielding and gas penetration into induced fractures.

2. EL836 EQUATION-OF-STATE

Adiabatic expansion of high explosive detonation products is often described with the Jones-Wilkins-Lee (JWL) equation-of-state. This empirical equation has been developed at Lawrence Livermore Laboratory (12) and is given by

$$P = A\left(1 - \frac{\omega}{R_1 \cdot V}\right)e^{-R_1 \cdot V} + B\left(1 - \frac{\omega}{R_2 \cdot V}\right)e^{-R_2 \cdot V} + \frac{\omega E}{V}$$

where

P = pressure (Pa)

V = relative volume (dimensionless v/v_o)

E = internal energy ($Pa \cdot m^3/m^3$)

A, B = linear coeffecients (Pa)

and R_1, R_2, ω = non-linear coefficients (dimensionless).

The equation-of-state parameters (i.e., A, B, R_1, R_2, ω and E_o) for EL836 have been experimentally determined by LLL for small, confined charges and are

$A = 2.174 \times 10^{11}$ Pa

$B = 2.908 \times 10^{9}$ Pa

$R_1 = 4.4$

$R_2 = 1.4$

$\omega = 0.16$

$E_o = 9.0 \times 10^{9}$ Pa $\cdot$ m^3/m^3

where E_o is the initial total available energy.

Dr. Coursen of duPont has indicated (13) that the JWL parameters obtained by LLL were obtained with charges and confinements which may have been too small for full reaction to occur. He suggests that for full-size shots in gas wells it might be better to assume that, aside from some cooled gas in the fractures, expansion occurs along the theoretical isentrope for complete chemical reaction with shifting equilibrium. Table 1 lists points on the isentrope of EL836, expanded from an initial density of 1490 kg/m^3, as calculated by duPont. Equivalent pressures, calculated using the JWL equation, are also listed for comparison.

As a part of the evaluation of EL836 for stimulating gas shale, two numerical calculations were performed to determine differences in explosive and shale behavior for each of the two equations-of-state. The STEALTH finite-difference code has a standard JWL equation-of-state option. Only the coefficients of the equation are required as input. An implicit time history of the JWL EL836 PV response, as calculated by STEALTH, is shown in Figure 1. For the isentropic expansion equation-of-state, a linear interpolation was performed between the discrete points of Table 1, to define the explosive expansion. An implicit time history of the isentropic EL836 PV response, using this interpolation, is also shown in Figure 1.

3. DEVONIAN GAS SHALE MODEL

As input to the STEALTH/CAVS computation, the material behavior of the gas shale requires appropriate constitutive equations describing

the elastic response, yielding and the plastic response, compressibility/compactability and tensile fracture. Since very little material data has been documented describing the dynamic response, of concern here, the descriptions used in these calculations are taken from static experiments or assumed from dynamic data obtained from experiments on similar rock types (e.g. oil shale). Table 2 summarizes the material descriptions used in these calculations. Figure 2 describes two Mohr-Coulomb type yield surfaces defining the gas shale yield stress as a function of pressure.

4. EL836 STIMULATION OF DEVONIAN GAS SHALE

4.1 Numerical simulation using STEALTH/CAVS

The STEALTH time-explicit finite-difference codes were used in this evaluation. Material description, boundary conditions and model geometry were defined to model the detonation of EL836 in an eight-inch diameter wellbore in Devonian gas shale. The calculations performed were one-dimensional and cylindrical, describing an infinitely long wellbore. Because the concern was not with wellbore end-effects or time-lapse effects as the explosive detonation propagates along the wellbore length and because these were primarily scoping calculations to assess general response and parameter sensitivity, one-dimensional computations were considered most cost-effective to describe the radial and circumferential response desired. Since the analysis was one-dimensional, pre-existing shale bedding planes (i.e., initial fractures) were not modeled. The shale model, therefore, represents a homogeneous isotropic initially unfractured rock mass. Figure 3 is a schematic of the one-dimensional cylindrical geometry model used in the calculations.

Of primary concern in these simulations was the degree of rock yielding and tensile fracture. Because EL836 is intended to develop abundant permanent gases as a significant part of the detonation reaction products, the influence of these gases on the fracture development was also an important aspect of numerical model.

The description of tensile fracture uses the CAVS (cracking and void strain) failure model. Details of this model can be found in Reference 11 and are summarized in Reference 4.

Crack Propping

In these calculations the jumbling sub-model of the more general CAVS constitutive description is utilized. The jumbling logic permits crack propping to model crack asperity mismatch or introduced proppants as cracks are reclosed as a result of compressive stress development across the opened crack. Details of this model are contained in Reference 4. A 20% bulking coefficient was used, providing a residual crack opening (i.e., void strain) which was at least 20% of the maximum achieved crack void strain. Previous calculation results (18) have shown the importance of crack propping in allowing borehole gas penetration into the induced fractures as the applied stress wave subsides, the stresses relax, becoming more compressive, and the cracks reclose.

Crack Pressurization

The gas pressurization sub-model of CAVS has been more recently developed. Conceptually the model attempts to describe the flow of gaseous detonation products or buffering liquids from the high pressure in the wellbore into the intersecting cracks. The flow model, as originally developed, was for a general three-dimensional representation of cracks that intersect with each other and with the borehole. Because cracks open and close in response to stress field changes, the model required a time-explicit description of the cracks that are open and those that are closed and knowledge of which cracks, for the purpose of gas flow, communicate with each other. A description of the intersecting crack system that is in communication with the high pressure fluid of the wellbore was the first requirement. Knowing the system of cracks into which gas could potentially flow, a description of the flow velocity and internal crack pressure was

required at each point in the crack system. Since the amount of gas or liquid available for penetration is finite, depending on the wellbore charge mass and the nature of the detonation reaction products, a limit was imposed on the mass that could flow and thus pressurize the crack system. Thus, the assistance provided by the internal pressurization in opening and extending cracks is limited to the available mass at a particular time.

A simplification of the model was used in the one-dimensional borehole calculations reported on here. This simplification, however, does not alter the basic physical description of fluid flow and pressurization. In these calculations, only the radial cracks are allowed to be pressurized. This does not represent a serious misrepresentation since the radially extending cracks are predominant in number, length and width, as compared to the circumferential, "spall type", cracks. Flow would also be presumed to be more difficult in these cracks.

The model is for transient gas flow and in its original form the equations are written for viscous conductance of a long, rectangular duct for flow of air at 20^{o} C. The only assumption for the model is that the flow is laminar viscous. A modified description was used by Wahi (19) in previous STEALTH calculations to simulate gas flow in a narrow gap between the fuel rod and adjacent cladding in a nuclear reactor. A detailed derivation of the required equations can be found in Appendix B of Reference 19. The concept of the model and the fundamental equations used in this model will be summarized below.

Fluid flow through a long, narrow, rectangular parrallelepiped is applicable, as a first approximation, to the flow of fluids from a wellbore into and through radially extending cracks. The CAVS description of cracks includes the crack's width, length and height (unit-height in one-dimensional geometry) required to describe the rectangular volume through which the gas/liquid is to flow. The volume of each crack, when summed over the total number of cracks for a given computational zone, describes the total volume into which fluids may potentially flow. Flow velocities in the cracks depend upon

the zone-to-zone pressure gradients and the conductance of the crack (rectangular duct). The conductance is essentially geometry and gas pressure dependent. Conductance can be written as dependent upon fluid viscosity and thus can be adjusted to model fluids of varying viscosity. This allows easy representation of most fluids used in wellbore stimulation treatments (e.g., water, oil, hot gases). A temperature dependent description of the fluid viscosity can also be described to model viscosity variations as the hot gases, of EL836 for example, cool upon entering the cracks. The temperature dependence of viscosity has not been used in these preliminary calculations.

The fluid flow velocity in the crack geometry described here can be defined and written in a modified form of Darcy's Law (21). Neglecting the elevation head term, small compared to the pressure head in this application, the flow velocity for fluid flow through a long, rectangular duct can be written as,

$$u = \frac{C}{A\bar{P}} (P_2 - P_1)$$

where

- u = average flow velocity relative to the crack over the crack cross-section area,
- A = crack cross-sectional area ($a * b$, below),
- $\bar{P}$ = average pressure in the crack,
- P_1, P_2 = pressures at points 1 and 2, usually assumed zone-to-zone crack pressures, (Pressure gradient is the fluid driving mechanism and pressures are linearly interpolated between points or zones), and
- C = conductance of the rectangular parallelepiped (crack).

The conductance for air at 20° C in a rectangular duct (20) is given by,

$$C = 0.26 \frac{a^2 b^2}{L} \bar{P} Y \quad \text{(liters/second)}$$

and when converted to SI units, becomes

$$C = (1.976 \times 10^3) \frac{a^2 b^2}{L} \bar{P}\, Y \quad (\text{meters}^3/\text{second})$$

where

a, b = sides of rectangle (meters), i.e., width and height of crack cross-section,

L = characteristic length of parallelepiped (meters), i.e., length of radial crack extending from wellbore,

$\bar{P}$ = mean pressure in-crack (Pascals), and

Y = function of ratio a/b (See Reference 20).

The conductance of fluids other than air through a rectangular duct can be expressed by,

$$C_{gas} = \frac{\eta^{\circ}_{air}}{\eta_{gas}(\theta)} C_{air}$$

where

η°_{air} = viscosity of air at 20° C, and

$\eta_{gas}(\theta)$ = viscosity of gas/liquid as a function of temperature.

The gas in the cracks is assumed to behave ideally. The equation-of-state is, therefore

$$P = R\rho\theta \tag{1}$$

where

R = universal gas constant,

ρ = mass density, and

θ = temperature.

Pressure changes are

$$dP = R\left[\rho d\theta + \theta d\rho\right]. \tag{2}$$

Changes in temperature were not considered for these calculations. Therefore, $d\theta = 0$. Density changes are

$$d\rho = d\left(\frac{m}{v}\right) = m\,d\left(\frac{1}{v}\right) + \frac{1}{v}\,dm \tag{3}$$

$$= \rho\frac{dv}{v} + \frac{1}{v}\left[(u_1 A_1\,dt)\rho_{2,1} + (u_3 A_3\,dt)\rho_{2,3}\right]$$

where

m = mass of gas in crack,

v = volume of gas in crack,

u_1, u_3 = velocities of gas at ends of crack segments, i.e., flow velocity in neighbor cracks,

A_1, A_3 = cross-section areas at ends of cracks segments, i.e., crack widths in neighbor cracks,

$\rho_{2,3} = \rho_3$: if $\rho_3 > \rho_2$
$= \rho_2$: if $\rho_3 < \rho_2$,

$\rho_{2,1} = \rho_2$: if $\rho_2 > \rho_1$
$= \rho_1$: if $\rho_2 < \rho_1$, and

dt = problem time step.

The index nomenclature can be represented by considering three consecutive zones (i.e., crack segments) as shown,

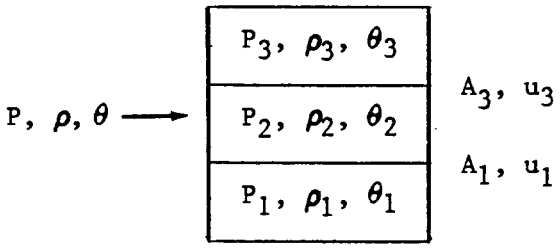

Substituting equation (3) into (2) yields, for $d\theta = 0$,

$$dP = P\left[-\frac{dv}{v} + \frac{u_3 A_3 dt}{v}\frac{P_3}{P_2} + \frac{u_1 A_1 dt}{v}\frac{P_1}{P_2}\right]$$

$$dP = P[Q]$$

Centering dP,

$$dP = \bar{P}[Q] = \left(P_{old} + \frac{dP}{2}\right)[Q]$$

Therefore,

$$dP = P_{old}[Q]/\left[1 - \tfrac{1}{2}[Q]\right]$$

and,

$$P_{new} = P_{old} + dP.$$

A more complete derivation including the effects of fluid temperature changes, flow in three-dimensional intersecting crack systems, and the difference equations required by STEALTH will be presented in future reports.

Features of the gas flow model used in internally pressurizing cracks can be summarized as follows:

- sections of cracks (defined by zone limits) are pressurized only if gases/fluids can flow into them, i.e., a segment of a crack will be pressurized if neighbor segments are pressurized and these neighbors have a continuous flow path to the gas/fluid source,

- fluid flow velocities are dependent on the pressure gradients between adjacent segments and the conductance of the crack segment,

- crack conductance is a function of crack geometry, particularly its width, the pressure in the crack and the fluid viscosity,

- fluid viscosity can be temperature dependent and modeled as such to represent cooling gas/liquids as they penetrate the cracks from the wellbore,

- a maximum flow velocity is defined which is less than the crack propagation speed,

- flow can be in either direction in a crack, depending on the zone-to-zone pressure gradients,

- gas availability can be time-dependent to describe the gas generation during explosive detonation,

- mass balance of the gases is maintained between the gas available in the wellbore and the gas penetrating the cracks. Total mass penetration of the gas is limited to the total available from the wellbore.

4.2 Calculation Results

Four one-dimensional cylindrical geometry (see Figure 3) numerical calculations were performed using the STEALTH finite-difference code. Tensile fracture of the shale was described using the CAVS failure model. Crack propping and internal pressurization were included in the STEALTH/CAVS computations. Two calculations were performed to assess the sensitivity of two different equations-of-state for EL836 and two calculations were performed to assess the influence on fracture development of rock yielding and internal crack pressurization.

In addition to the tensile fracture description provided by CAVS, the shale material properties description included representative compressibility and yield models. These are summarized, along with the other material properties of shale, in Table 2. All properties were assumed isotropic describing a homogeneous initially unfractured (i.e., bedding planes were not modeled) rock mass.

Comparison of EL836 Stimulation Using Two Different EL836 Equations-of-State

As described in Section 2, two different descriptions of the EL836 detonation response were considered for evaluation. Adiabatic expansion

was modeled using first the JWL equation-of-state and second the duPont calculated isentropic equation-of-state. Table 1 presents a comparison of calculated pressures for discrete points of relative volume. Figure 1 illustrates the two PV responses. The isentrope response of the figure is incremental between the points defined in Table 1. A linear interpolation was used in the calculations to define the intermediate pressures. Note that the calculated pressures fall more gradually than the JWL description, as suggested by Dr. Coursen. The wellbore pressure-time histories (used with the normal strength yield model of Figure 2) for the two EL836 equations-of-state are shown in Figure 4. Note also the maintained higher pressure for longer duration in the duPont description of EL836.

Figures 5a and 5b are radial stress histories at the wellbore wall (i.e., first rock zone in the mesh). Figures 6a and 6b are circumferential stress histories at the wellbore wall. Note that the hoop stresses immediate to the wellbore are never tensile to induce fracture. Figures 7a and 7b and Figures 8a and 8b are equivalent radial and circumferential stress histories at a distance of 2 meters from the wellbore center. At this distance, tensile hoop stresses are significant (Figures 8a and 8b) and are reflected in the tensile cracking that occurs.

Wellbore expansion for the two calculations is illustrated in Figures 9a and 9b. Due to the higher pressures for longer duration, wellbore expansion is more pronounced for the duPont EL836 EOS calculation. The degree of rock yielding is shown in Figure 10. The ordinate parameter is essentially a measure of stress adjustment performed in accordance with the Prandt-Reuss flow rule when the von Mises yield criterion exceeds the defined yield stress. The degree of yielding is defined as

$$DY = 1/ADJ$$

where ADJ is the adjustment made to the deviatoric stresses when plastic flow occurs. ADJ ranges from a very small number to 1 and

equals

ADJ = YLD/YSTN

where YLD is the yield strength of the rock (defined as a function of pressure in Figure 2), and YSTN is the von Mise yield stress. Figure 10a and 10b, when compared, show increased yielding (by an order of magnitude in this description) for the duPont EL836 EOS as compared to the JWL EL836 EOS description. A more realistic parameter for this comparison might have been selected, such as the plastic strains.

Results of the CAVS fracture computations are shown in Figures 11 and 12 and Figures 15 through 24. Comparison should be made between Figures 11 and 12, which show the void strain distributions as a function of radial distance from the wellbore. Significant differences are not apparent in a general sense considering the smallness of the void strain (generally less than 0.1%). Note the opening and closing of the cracks in Figure 11 at radial distances of less than a meter. Note also that void strain, under the code convention, is more negative with increased crack opening.

The distribution of induced tensile fracturing is shown in Figures 15 through 19, for the JWL EL836 EOS description, and in Figures 20 through 24, for the duPont EL836 EOS description. The figures appear to show crack intersection with the wellbore. There is however a very small zone near the wellbore in which no cracking has occurred. The sensitivity of the plotter used to prepare these figures prohibits showing this feature. Comparisons should be made between the two sets of figures at equivalent calculation times. The outside boundary of the computation model is at about 25 meters. The outside boundary of the CAVS fracture plots is at 14 meters. In general, the differences between these two calculations are minor, although crack numbers are somewhat greater at later times for the duPont description of EL836. Note that in both cases, yielding immediately around the wellbore has prohibited fracture development and thus wellbore gas intrusion into the outer-lying cracks. The zone of yielding without fractures becomes quite

small as time progresses, but the "dam" that separates the wellbore gases from the cracks is not broken with computations to 3 milliseconds for the normal strength yield description. Realistic analysis of this fine zone would have to account for the distortional strains, shearing, crushing and pre-cracks resulting from drilling. Computational pre-cracking the initial rock zones can overcome this difficulty to enable gas penetration into the cracks. This has been performed and the results are discussed below.

Assessment of the Effect of Yielding and Crack Pressurization in EL836 Stimulation

As indicated above the effect of wellbore yielding can have significant detrimental effects on the fracture development in EL836 stimulation treatments. The calculations described above use a yield model that is considered representative. Stimulating a wellbore with EL836 in rock whose behavior is similar to the material properties used in the above described calculations would be subjected to extensive plastic flow, particularly near the wellbore. A one-dimensional calculation, using the duPont EL836 EOS, was performed with identical shale material properties as those used above except that a higher yield strength was modeled (Figure 2). The intent was to lessen the plastic flow, allowing higher tensile stresses to develop and induce fracturing in the rock immediate to the wellbore wall. The additional fracturing was expected to enable gas communication between the wellbore and the cracks. The computation was performed to 5 milliseconds (2 milliseconds longer than previous EL836 calculations). At early times in the computation, rock yielding prohibited tensile fracture. For example, at a time of ½ millisecond, the plastic region around the wellbore extended to approximately 0.3 meter (three borehole radii). As the computation time increased and the pressure pulse in the wellbore subsided, tensile cracking advanced from the outer region of the plastic zone towards the borehole. At a time of 3/4 milliseconds, the unfractured portion of the plastic zone had reduced to two borehole radii. Tensile fracture stopped advancing towards the wellbore after about 1 millisecond and

did not break through, even at 5 milliseconds. The effect of internal crack pressurization was, therefore, not observed. The calculation using the higher strength yield model, however, did show additional crack development, as compared to the low yield strength computation (Figures 20 through 24). These results are not described in the tables and figures of this report, although in summary, in the high strength calculation, cracking extended to approximately 12 meters as compared to 10 meters in the normal (lower) strength calculation. Only minor differences were observed in comparing the void strain versus radial distance distribution.

As a means of allowing gas penetration, the first zone of rock adjacent to the wellbore was pre-cracked with defined finite but small void strain. The pre-crack void strain was defined small to eliminate the effect of borehole-grooving and "groove" (crack) extension resulting from internal pressurization by wellbore gases. The final calculation was performed using the pre-cracking and run to a time of 5 milliseconds. In the computation, a region of plastic yielding again developed, although it was minimized by using the higher strength yield model. After a time of about 3/4 millisecond, tensile cracks had developed through the zone of plastic flow to the pre-cracked zone, enabling gas penetration from the wellbore into the radial crack system that had developed by the passing stress wave. The results of this calculation are shown in Figures 5c (radial stress-time history at the wellbore wall), 6c (hoop stress-time history at the wellbore wall), 7c (radial stress-time history at 2 meters from the wellbore), 8c (hoop stress-time history at 2 meters from the wellbore), 9c (wellbore expansion, radius-time history), 13 (void strain vs radial distance at 1, 2 and 3 milliseconds), and 14 (crack pressure vs radial distance at 1, 2 and 3 milliseconds). It is significant to note the order-of-magnitude increase in the void strain in the radial crack system when the cracks are internally pressurized. Compare Figures 11 and 12 with Figure 13. The comparison of crack opening (represented by the void strain) is even more pronounced in Figure 33, which illustrates the results of two calculations after 5 milliseconds with and without gas

pressurization. Figure 14 shows the crack pressure profiles at 1, 2, 3, 4, and 5 milliseconds. The peak pressure in the radial crack system drops as the borehole pressure drops and the radial extent of gas penetration and crack pressurization increases with time.

The pressure profile in a continuous open fracture system would be expected to be low and constant when equilibrium is reached. After 5 milliseconds (calculation time) the pressure profile is somewhat constant close to the wellbore, yet at the furthest radial extent (approximately 1.2 meters) of gas penetration the pressure profile is not constant. This suggests that gas flow and pressurization of the extending cracks is not complete at this time and quasi-static, late-timeaffects have yet to be accounted for. A complete simulation would thus require a longer time calculation or restarting at 5 milliseconds and extending the computation to perhaps several seconds to account for the quasi-static affects. It is also likely that the damage immediately around the wellbore will "trottle" the gas flow and significantly reduce the near wellbore "source" pressure that the crack system experiences.

5. SUMMARY

Results of a computational evaluation of the EL836 explosive in stimulating Devonian gas shale suggest the following:

- Extensive plastic yielding will occur in a region immediate to the borehole. For typical gas shale, this region extends to about three borehole radii.

- Extensive tensile fracture will occur in a region that begins at the outer boundary of plastic deformation and terminates at more than 100 borehole radii (approximately 10 meters).

- Without a mechanism of near-wellbore fracture, such as crushing

or pre-cracking during drilling or intentional borehole grooving, the plastic flow that occurs adjacent to the wellbore causes stress redistributions which prohibit early-time (less than a millisecond) tensile fracture immediate to the wellbore and thus prohibits gas penetration from the wellbore into the crack system.

- The barrier that the near-wellbore plastic zone presents to gas flow from the wellbore is reduced in radial dimension as time increases. It would thus be expected that at late times in the EL836 stimulation treatment breakthrough would be achieved, enabling gas penetration into the crack system.

- Natural fractures in the wellbore wall or cataclysmic deformation and fracture adjacent to the wellbore, as a result of the explosive detonation, will likely assist in breaking down the barrier to gas flow, and thus enable early-time gas penetration.

- Very significant enhancement is achieved in the EL836 stimulation treatment when gases penetrate the stress-wave induced radial cracks. Crack opening is increased by an order-of-magnitude and crack extension is improved.

- Only minor differences were observed in the EL836 stimulation effects when comparison is made between two different explosive equations-of-state.

REFERENCES

1. McHugh, S.L., DeCarli, P.S., and Keough, D.D., "Small-Scale Experiments with an Analysis to Evaluate the Effect of Tailored-Pulse-Loading on Fracture and Permeability," Quarterly Progress Report 2, SRI Project PYU-8621, April 1980, SRI International, Menlo Park, California.

2. Fourney, W.L., Holloway, D.C., and Barker, D.B., "Pressure Decay in Propagating Cracks," January 1980, Prepared for Morgantown Energy Technology Center by Photomechanics Laboratory, Mechanical Engineering Department, University of Maryland, College Park, Maryland.

3. Schmidt, R.A., "*In Situ* Testing of Well Shooting Concepts," Reports 1, 6, 7 and 9, Sandia Laboratories, Albuquerque, New Mexico.

4. Barbour, T.G., Maxwell, D.E., and Young, C., "Numerical Model Developments for Stimulation Technologies in the Eastern Gas Shales Project," January 1980, Task Technical Report under Contract EY-78-C-21-8216 for Morgantown Energy Technology Center. Prepared by Science Applications, Inc., Fort Collins, Colorado.

5. Moore, E.T., Mumma, D.M., and Seifert, K.D., "Dynafrac-Application of a Novel Rock Fracturing Method to Oil and Gas Recovery," April 1977, Physics International Report 827, San Leandro, California.

6. Fitzgerald, R. and Anderson, R., "Kine-frac - A New Approach to Well Stimulation," November 1978, ASME Paper 78-PET-25, ASME Technology Conference and Exhibition, Houston, Texas.

7. Warpinski, N.R., Schmidt, R.A., and Cooper, P.W., "High-Energy Gas Frac: Multiple Fracturing in a Wellbore," June 1979, Proc. 20th U.S. Sym. Rock Mech., Austin, Texas.

8. Coffey, C.E., E.I. duPont de Nemours and Company, Wilmington, Delaware, letter to C.A. Komar, Morgantown Energy Technology Center, Morgantown, West Virginia, November 1978.

9. Coursen, D.L., E.I. duPont de Nemours and Company, Martinsburg, West Virginia, letter to T.G. Barbour, Science Applications, Inc., Fort Collins, Colorado, July 1980.

10. Hofmann, R., "STEALTH, A Lagrange Explicit Finite-Difference Code for Solids, Structural and Thermohydraulic Analysis," EPRI NP-176-1, Electric Power Research Institute, Palo Alto, California, April 1978. Prepared by Science Applications, Inc., San Leandro, California.

11. Maxwell, D.E., "The CAVS Tensile Failure Model," Internal Report SATR 79-4, April 1979. Science Applications, Inc., San Leandro, California.

12. Lee. E.L., Hornig, H.C., and Kury, J.W., "Adiabatic Expansion of High Explosive Detonation Products," UCRL-50422, May 1968, Lawrence Radiation Laboratory, University of California, Livermore, California.

13. Coursen, D.L., E.I. duPont de Nemours and Company, Martinsburg, West Virginia, personnel communique, April 1980.

14. Hanson, M.E., Emerson, D.O., Heard, H.C., Shaffer, R.J., and Carlson, R.C., "Quarterly Report: The LLL Massive Hydraulic Fracturing Program for Gas Stimulation, July-September 1976," UCRL-50036-76-3, October 25, 1976, Lawrence Livermore Laboratory, University of California, Livermore, California.

15. Hanson, M.E., Heard, H.C., Hearst, J.R., and Shaffer, R.J., "LLL Gas Stimulation Program, Quarterly Progress Report, October through December 1976," UCRL-50036-76-4, February 15, 1977, Lawrence Livermore Laboratory, University of California, Livermore, California.

16. Schott, G.L., "Stimulation and Characterization of Eastern Gas Shales, April-June 1978," LA-7654-PR, December 1978, Los Alamos Scientific Laboratory, Los Alamos, New Mexico.

17. Olinger, B., "Determining the Dynamic Properties of Devonian Gas Shale," Proc. 20th U.S. Sym. Rock Mech., June 1979, Austin, Texas.

18. Barbour, T.G., unpublished notes, Science Applications, Inc., Fort Collins, Colorado.

19. Wahi, K.K., "One and Two-Dimensional Simulations of Fuel Pin Response," June 1979, SAI-FR-039, San Leandro, California. To be published by EPRI, Palo Alto, California.

20. Condon, E.U. and Odishaw, H. (eds), Handbook of Physics, 1958, McGraw-Hill Book Co., Inc., New York, New York, (pp. 5-78, 5-79).

21. Darcy, H., Les Fontaines Publiques de la Ville de Dijon, V. Dalmont, Paris, 1865.

Table 1

EL836 EQUATION-OF-STATE

Relative Volume	Pressure (Pa)	
	Isentrope*	JWL†
0.7674 (CJ)	115.49×10^8 (CJ)	97.97×10^8
1.000	53.57	46.47
1.249	30.80	23.65
1.629	16.67	11.82
2.248	8.671	7.239
3.318	4.495	2.973
5.212	2.343	2.606
8.606	1.188	1.532
14.830	0.628	0.882
26.233	0.345	0.496
47.065	0.174	0.276

* Calculated by E.I. duPont de Nemours and Co. (13)

† Calculated using JWL Equation-of-State (12)

Table 2

DEVONIAN GAS SHALE MATERIAL PROPERTIES

		Reference
Mass Density (ρ_o)	2550 kg/m^3	(17)
Isotropic Elastic		
Bulk Modulus (K)	2.6×10^{10} Pa	(17)
Shear Modulus (G)	2.0×10^{10} Pa	(17)
Isotropic Plastic		
Yield Stress (Y)	$Y = \sqrt{4\alpha P} + \beta P + \gamma$ (Pa)	(14,15,16)
	Baseline / High Strength	
	$\alpha = 3.7 \times 10^7$ Pa / $\alpha = 6.0 \times 10^7$ Pa	
	$\beta = -0.30$ / $\beta = -0.30$	
	$\gamma = 6.0 \times 10^7$ Pa / $\gamma = 8.0 \times 10^7$ Pa	
Flow Rule - non-associated Prantl-Reuss as defined in STEALTH		
CAVS Tensile Failure		
Virgin Tensile Strength (σ_{t_o})	1.034×10^7 Pa	(17)
Ratio of Initiation-to-Propagation Tensile Strengths	2.0	
Tensile Modulus (TK)	3.44×10^9 Pa	
Strengths adjusted according to the degree of cracking		
$\sigma_t = C^{NTC}(\sigma_{t_o})$	C = 1.05	
	NTC = number of zone through cracks	
Maximum permanent gas availability for penetration into cracks	24 moles/kg charge	
In Situ Stresses		
Isotropic (typical)	6.895×10^6 Pa	
Initial Joints (bedding planes)	No	

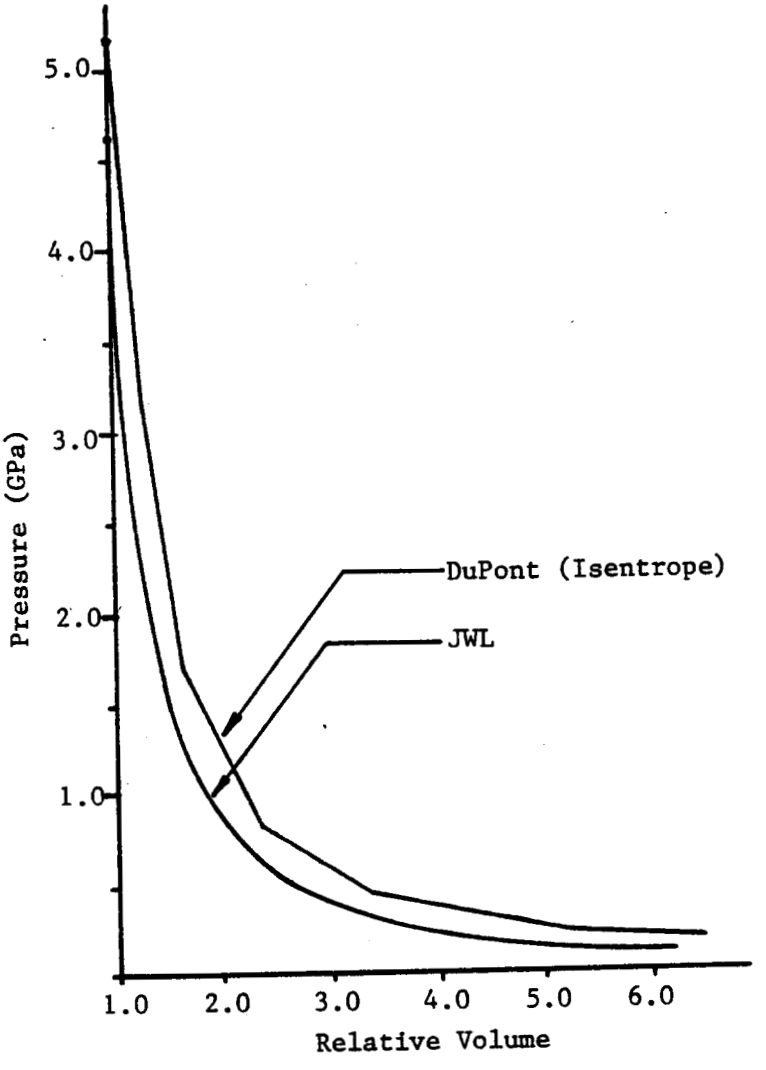

Figure 1. EL836 Equation-of-State

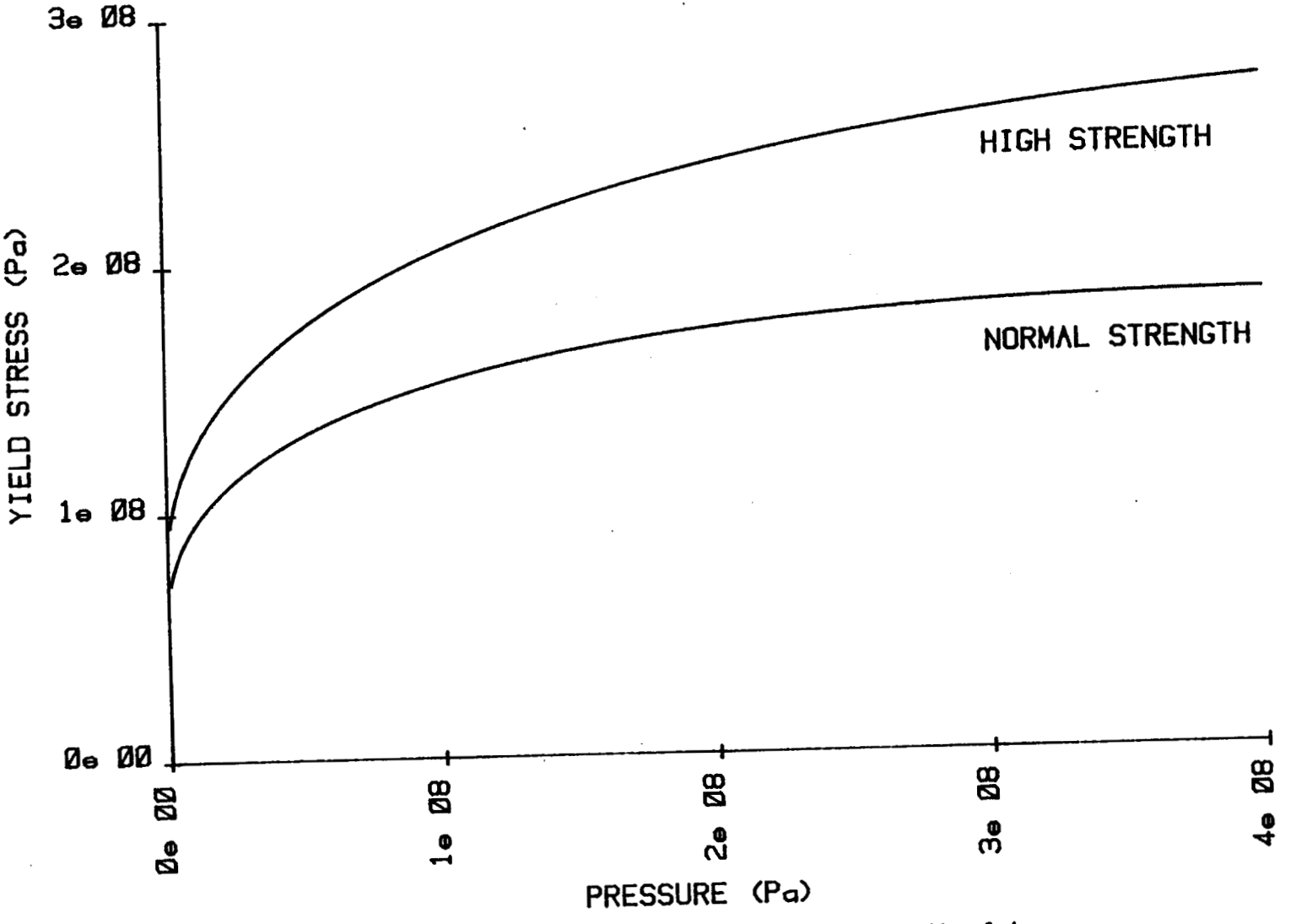

Figure 2. Devonian Gas Shale Yield

SAI JULY 1980

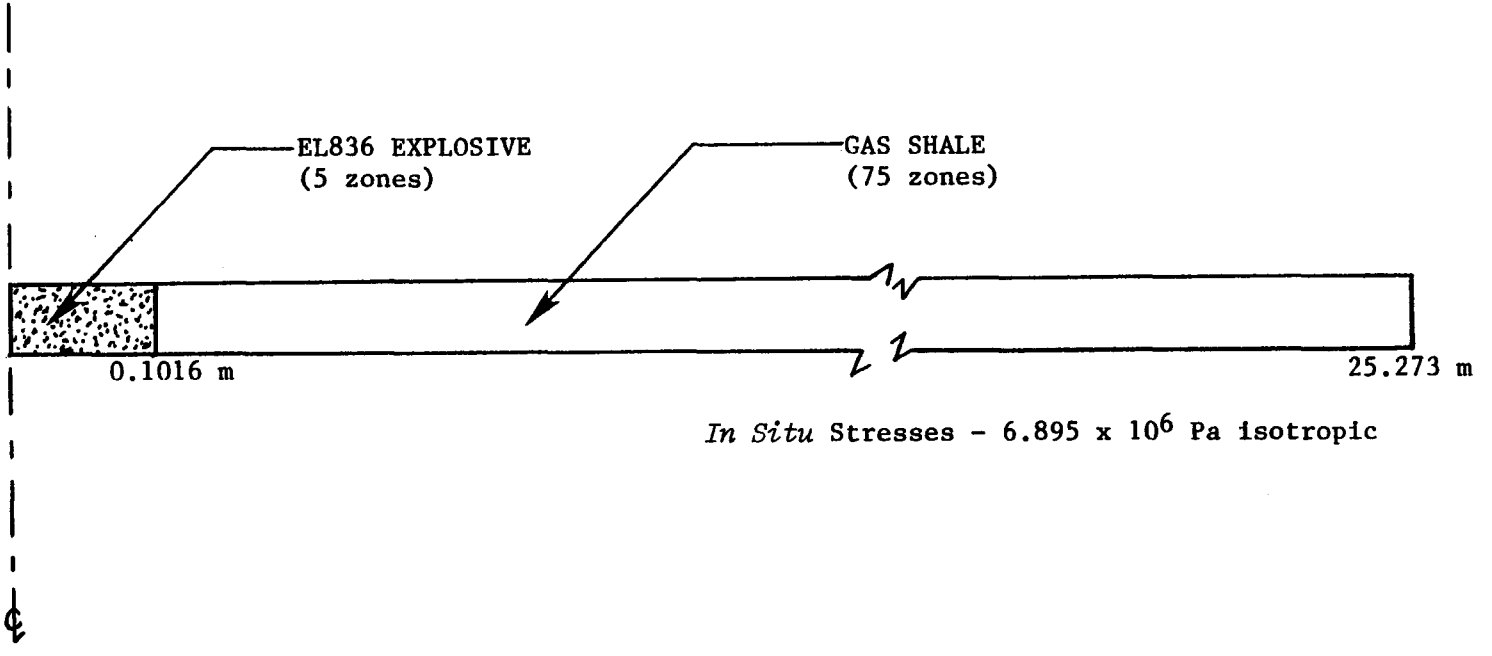

Figure 3. One-dimensional cylindrical geometry model for the evaluation of EL836 stimulation of gas shale.

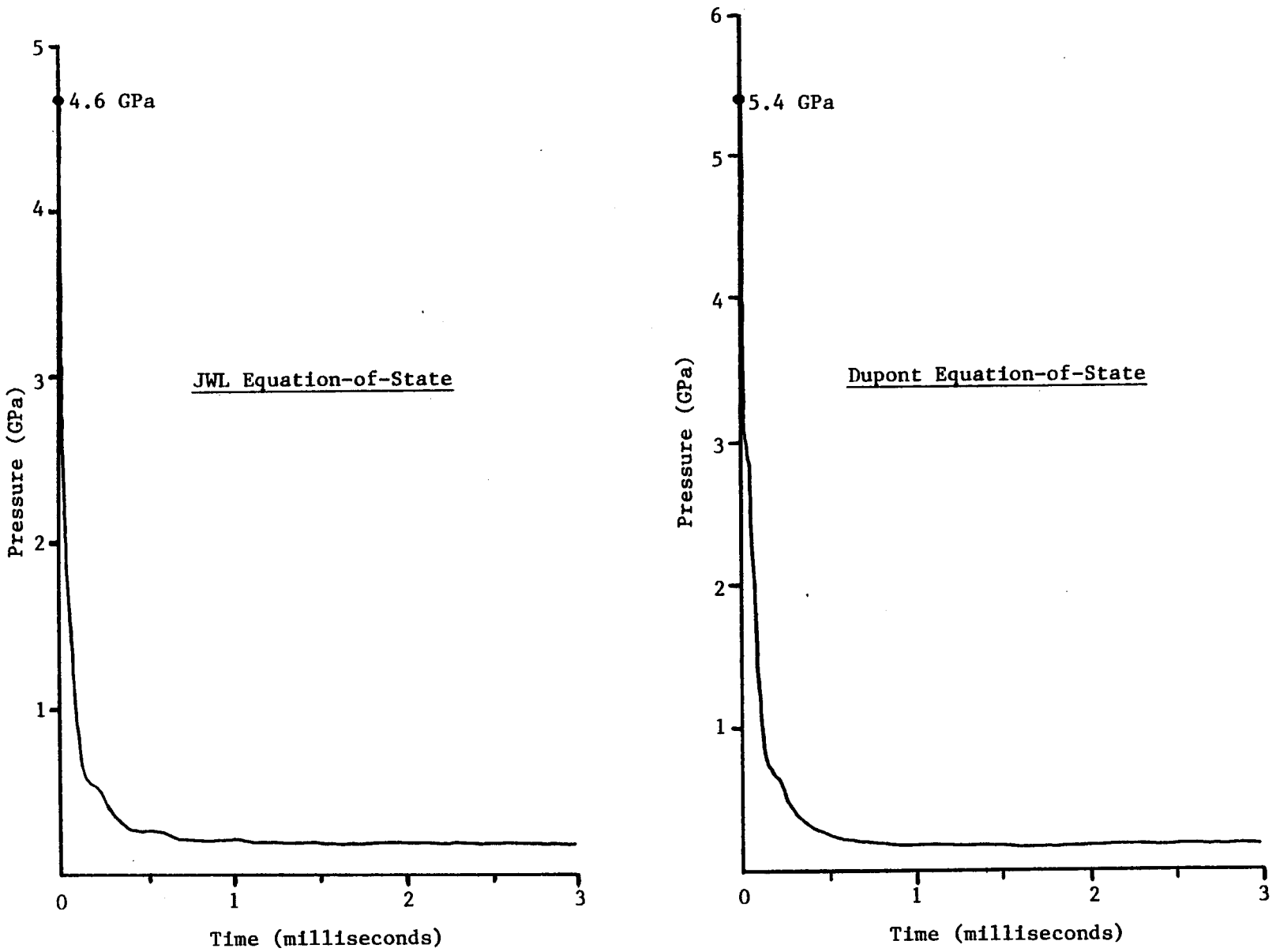

Figure 4. Borehole Pressure-Time History

JWL EL836 EOS
NORMAL ROCK STRENGTH

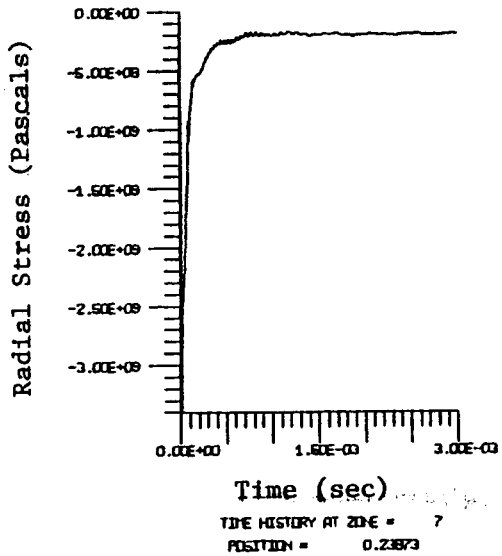

(a)

DUPONT EL836 EOS
NORMAL ROCK STRENGTH

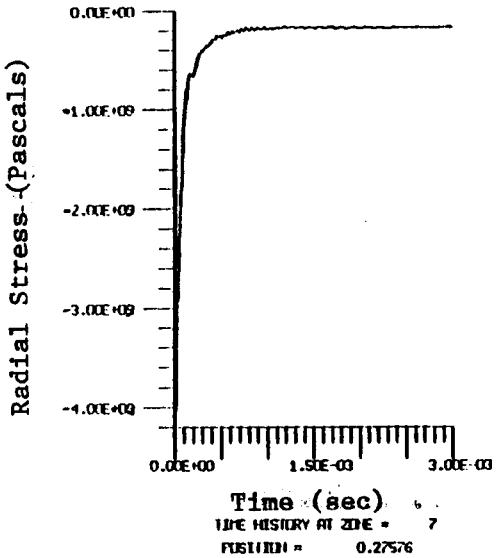

(b)

DUPONT EL836 EOS
HIGH ROCK STRENGTH
CRACK PRESSURIZATION

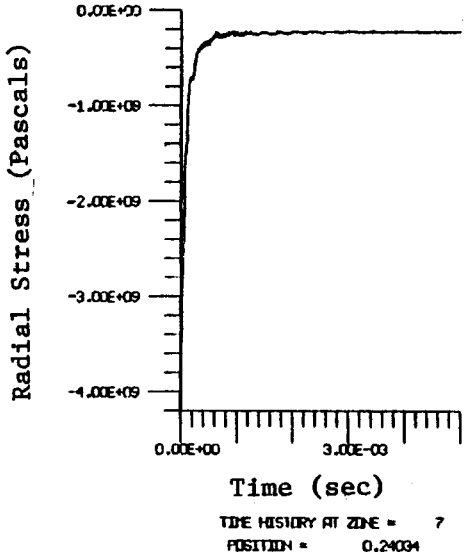

(c)

Figure 5. Radial Stress-Time History at Wellbore Wall

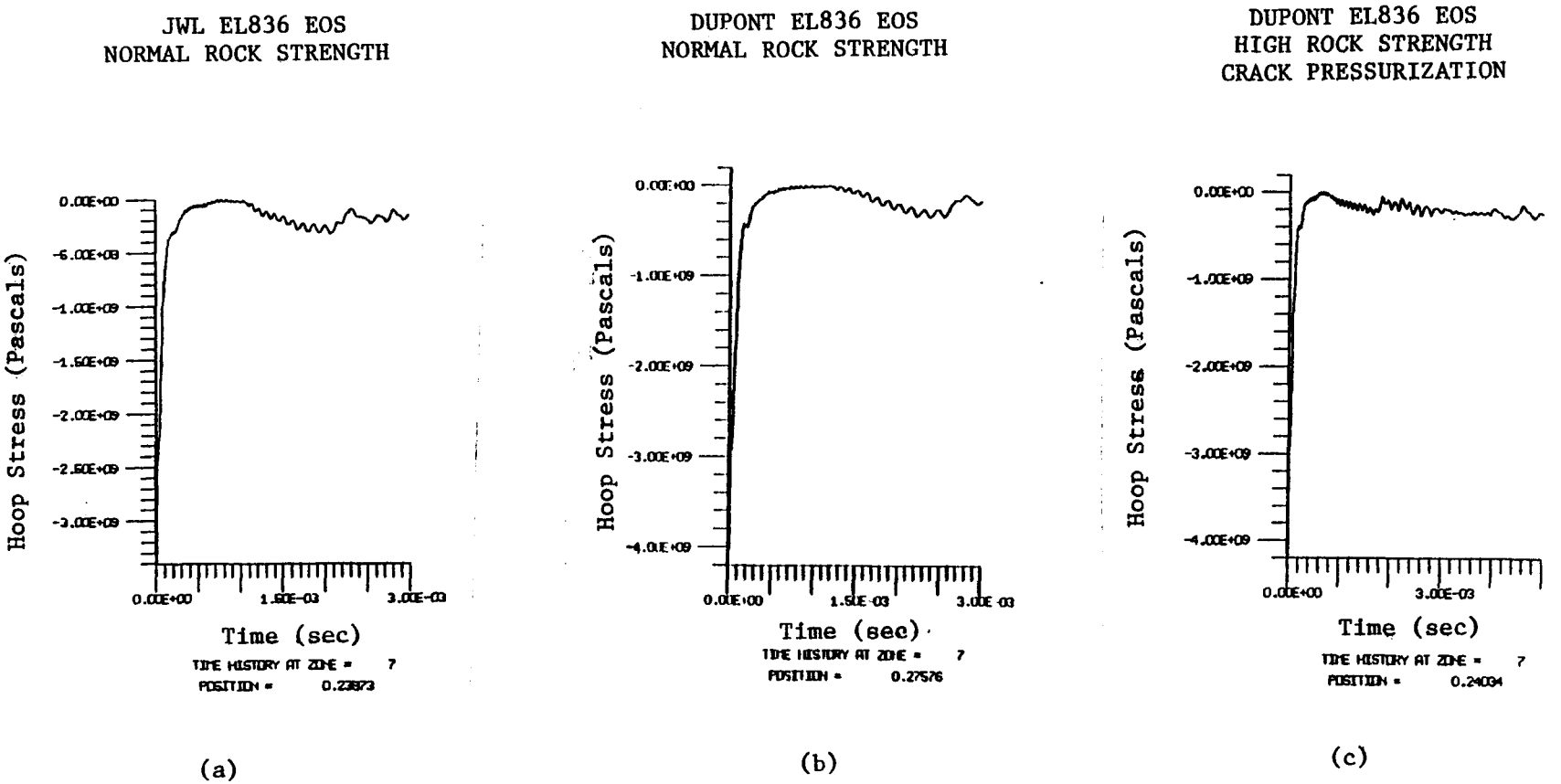

Figure 6. Hoop Stress-Time History at Wellbore Wall

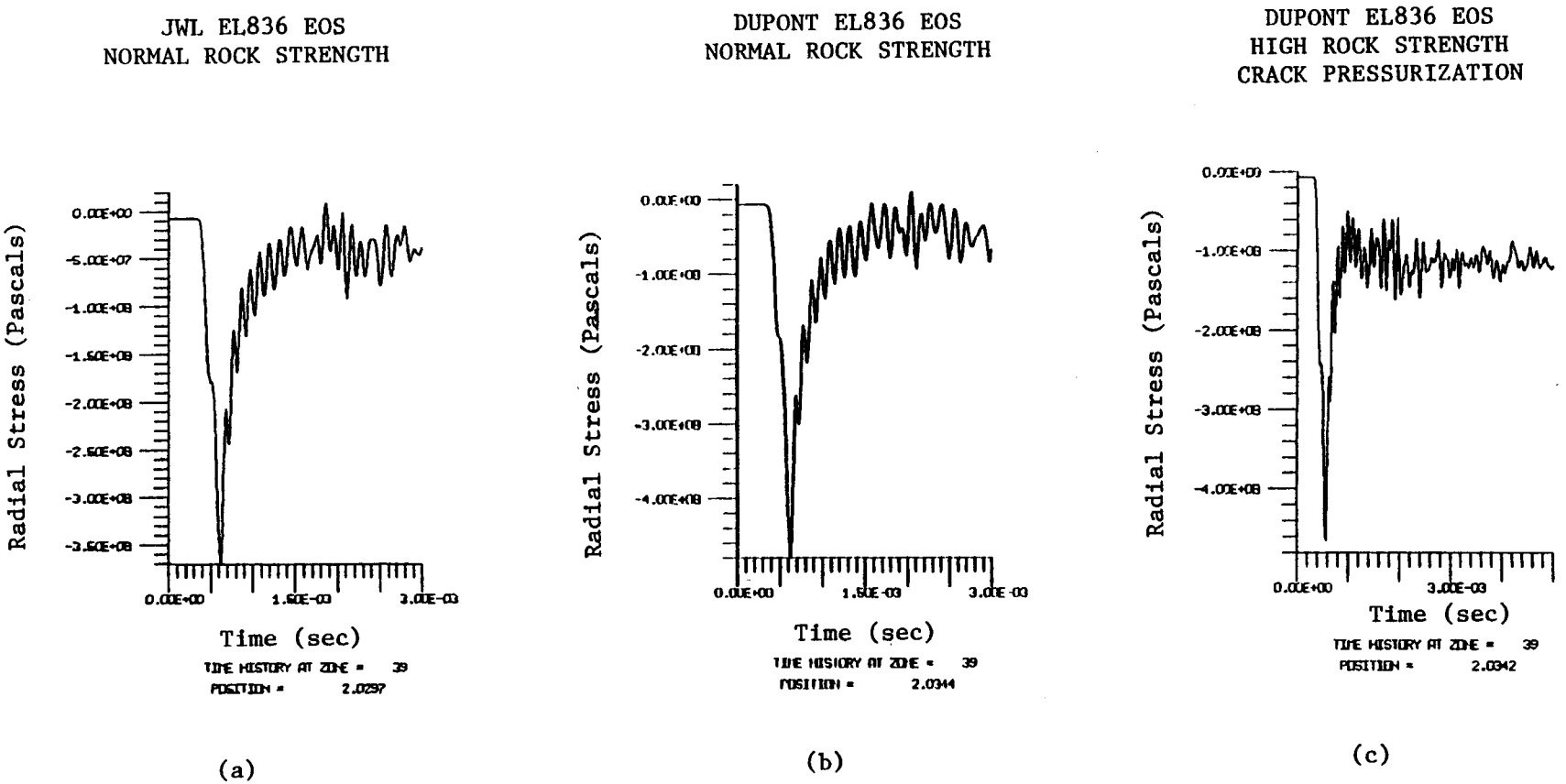

Figure 7. Radial Stress-Time History at 2 meters from Wellbore

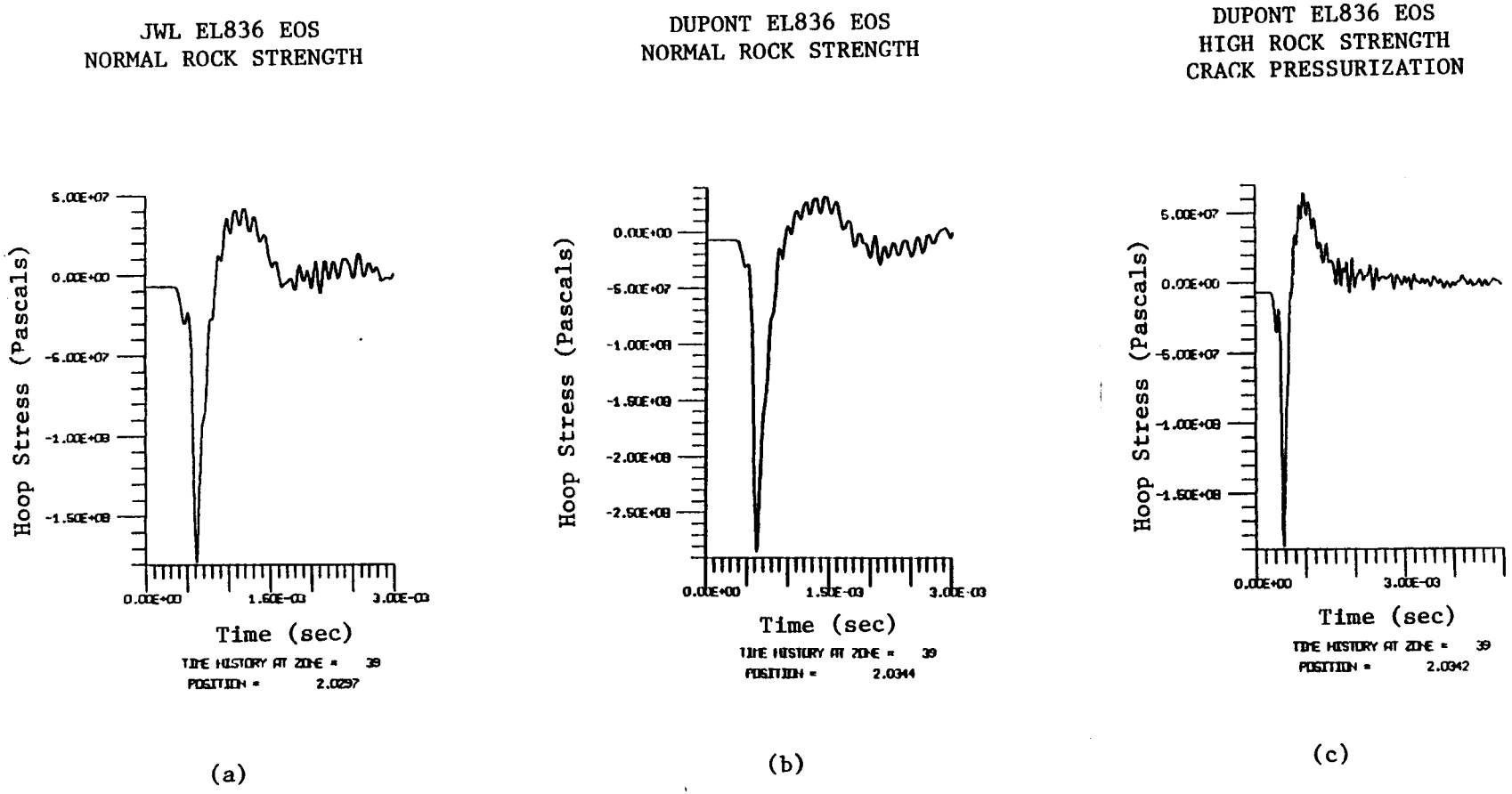

Figure 8. Hoop Stress-Time History at 2 meters from Wellbore

JWL EL836 EOS
NORMAL ROCK STRENGTH

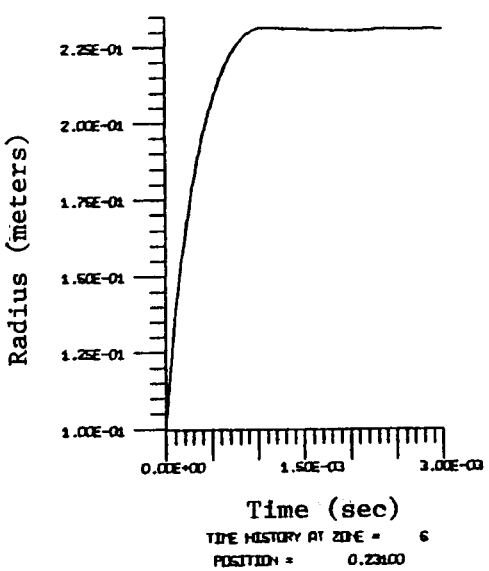

(a)

DUPONT EL836 EOS
NORMAL ROCK STRENGTH

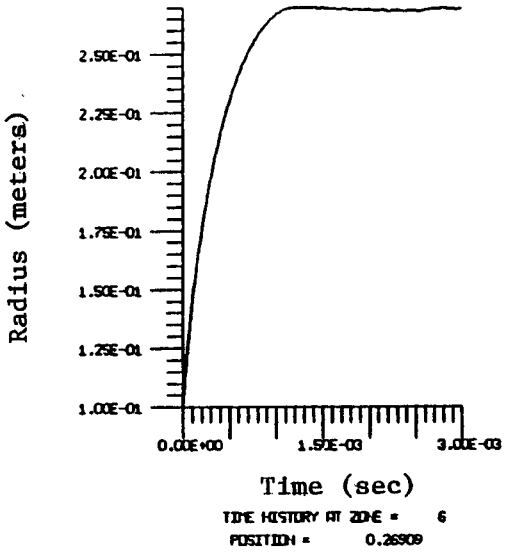

(b)

DUPONT EL836 EOS
HIGH ROCK STRENGTH
CRACK PRESSURIZATION

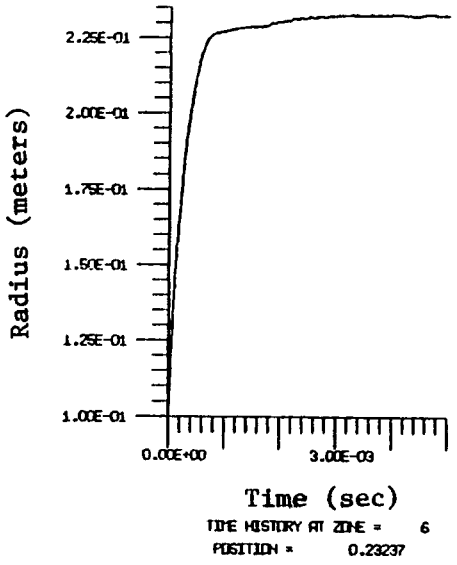

(c)

Figure 9. Wellbore Expansion, Radius-Time History

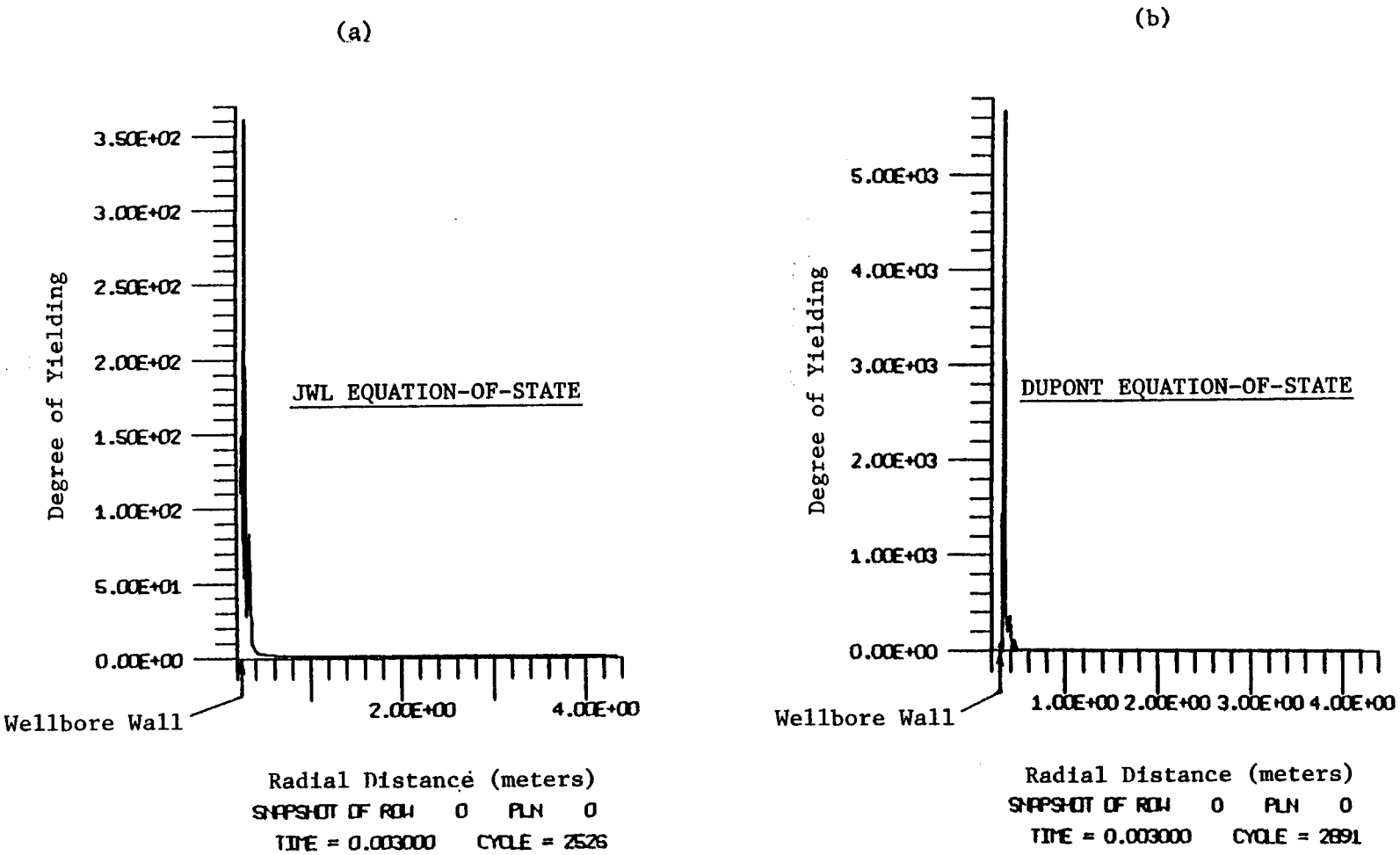

Figure 10. Degree of Rock Yielding vs Radial Distance

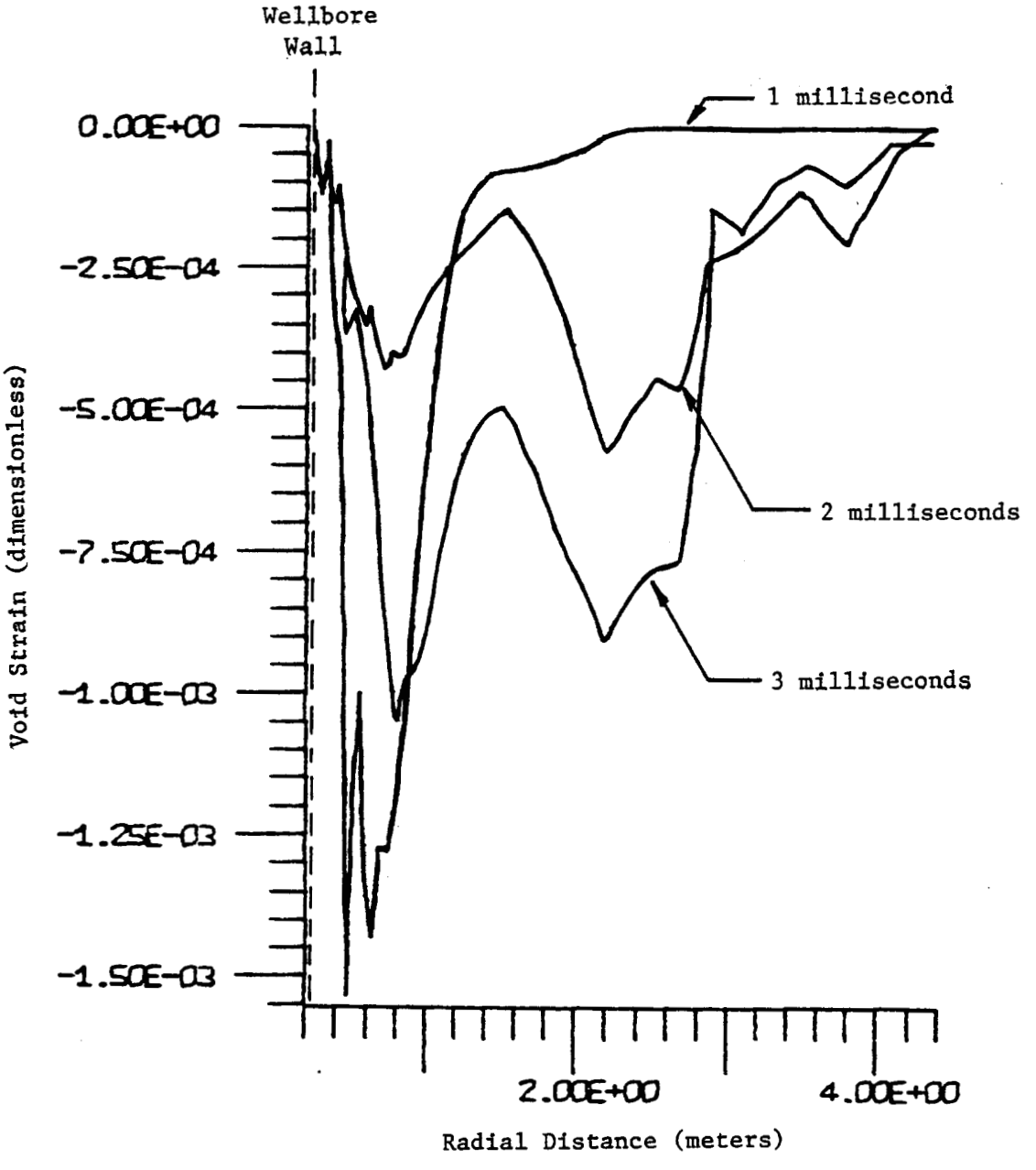

Figure 11. Void Strain vs Radial Distance, EL836 Stimulation using JWL EOS

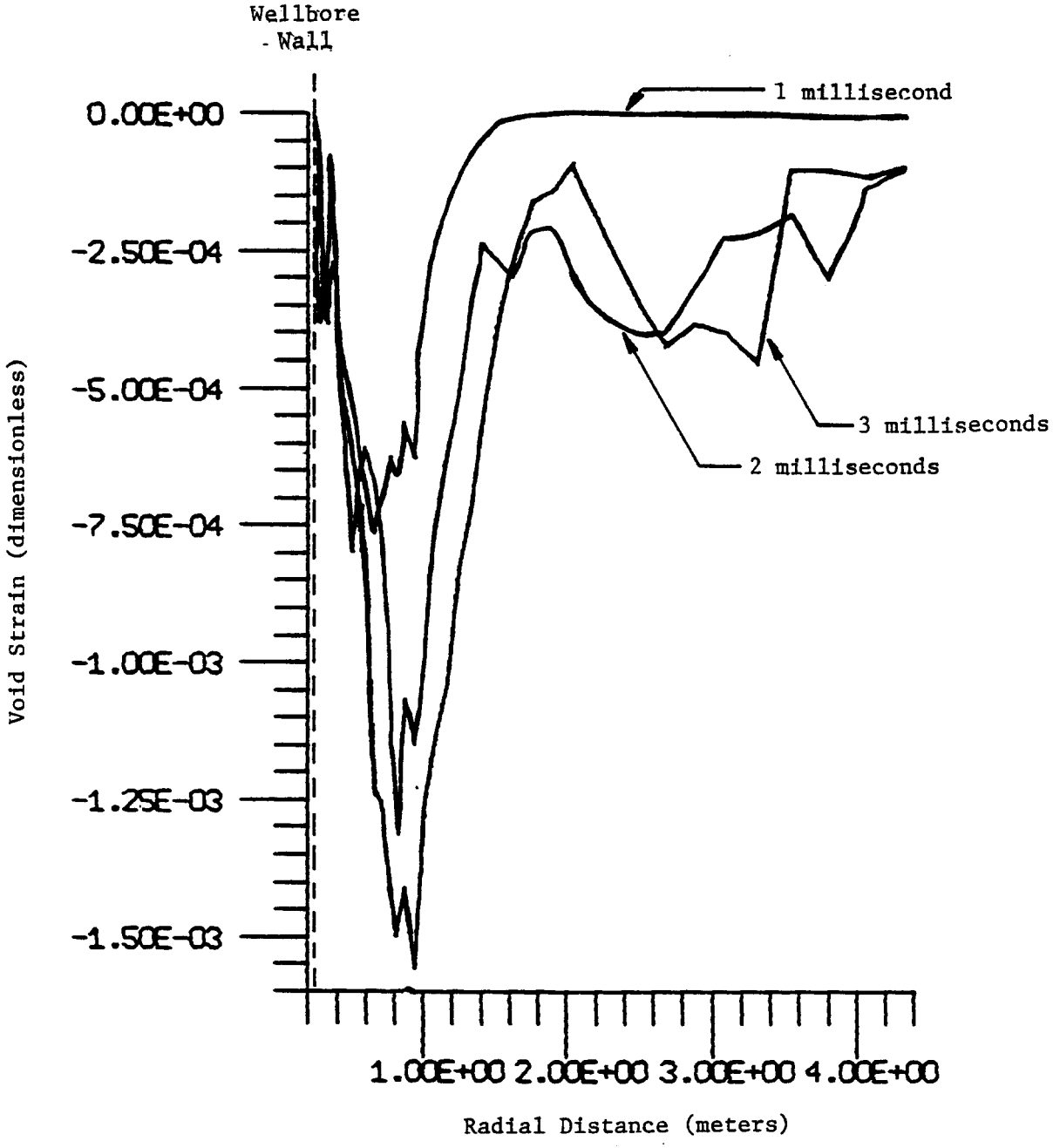

Figure 12. Void Strain vs Radial Distance, EL836 Stimulation using duPont EOS

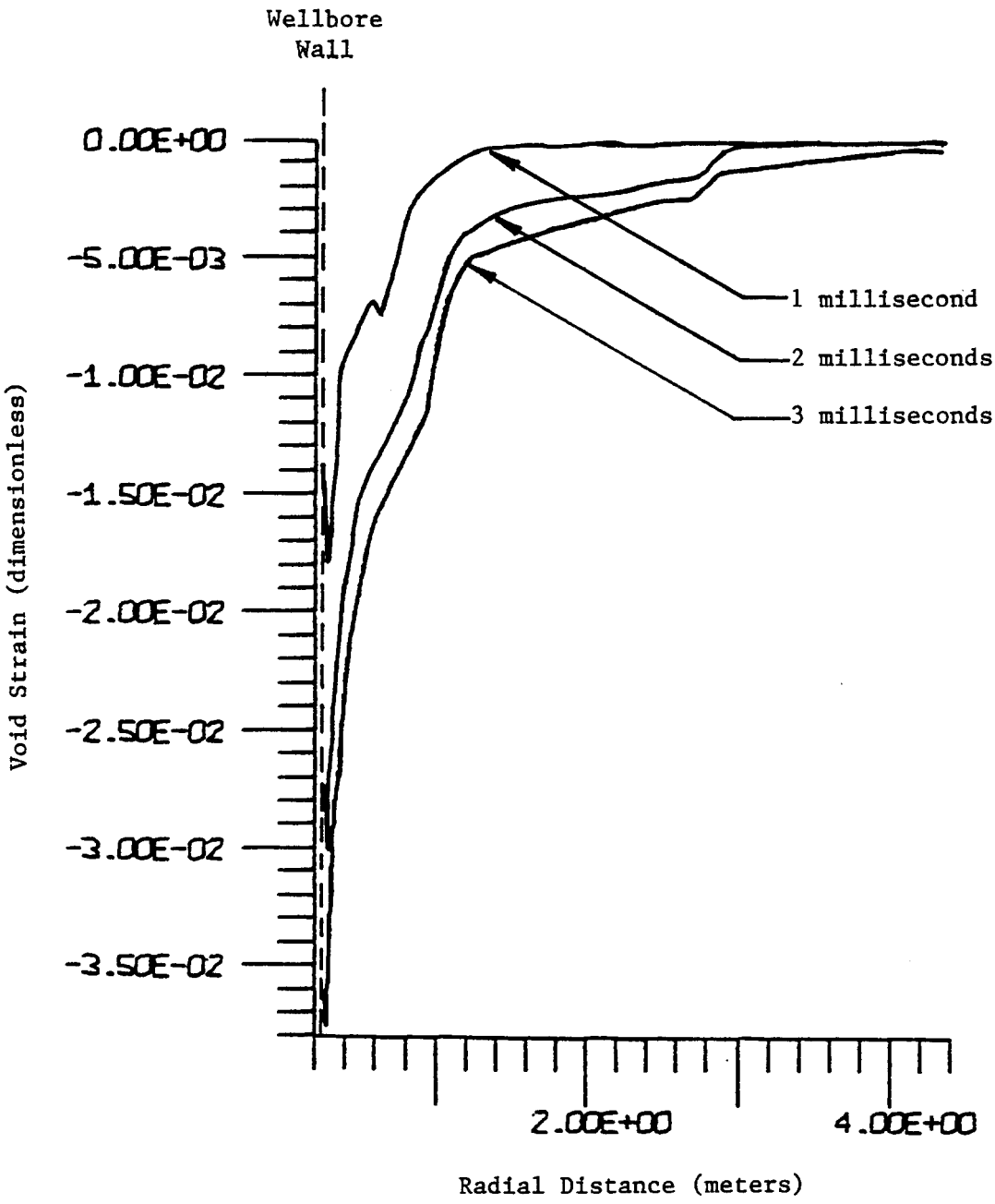

Figure 13. Void Strain vs Radial Distance, EL836 Stimulation using duPont EOS, with high strength rock and crack pressurization

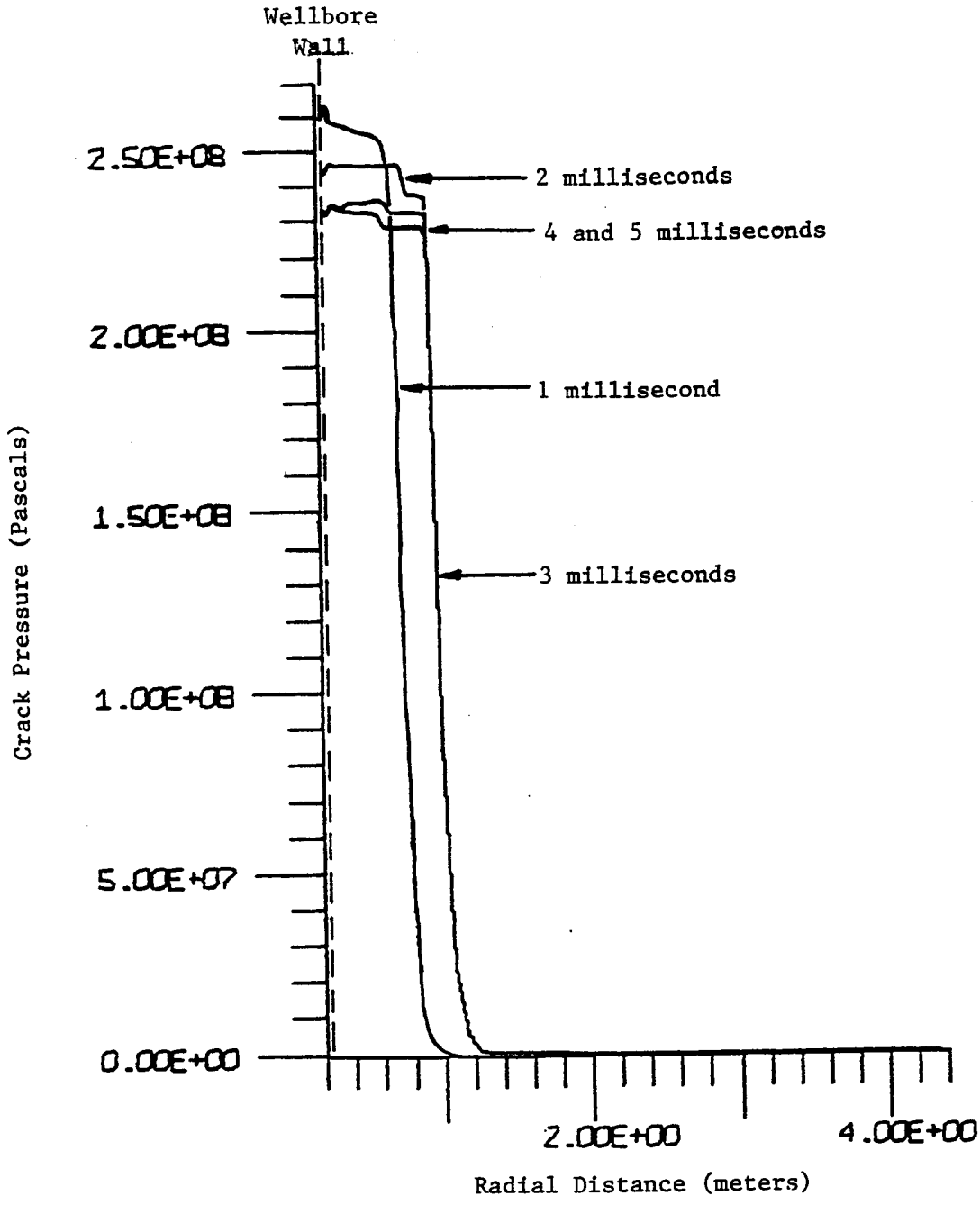

Figure 14. Crack Pressure vs Radial Distance, High Rock Strength, Pre-cracked Wellbore

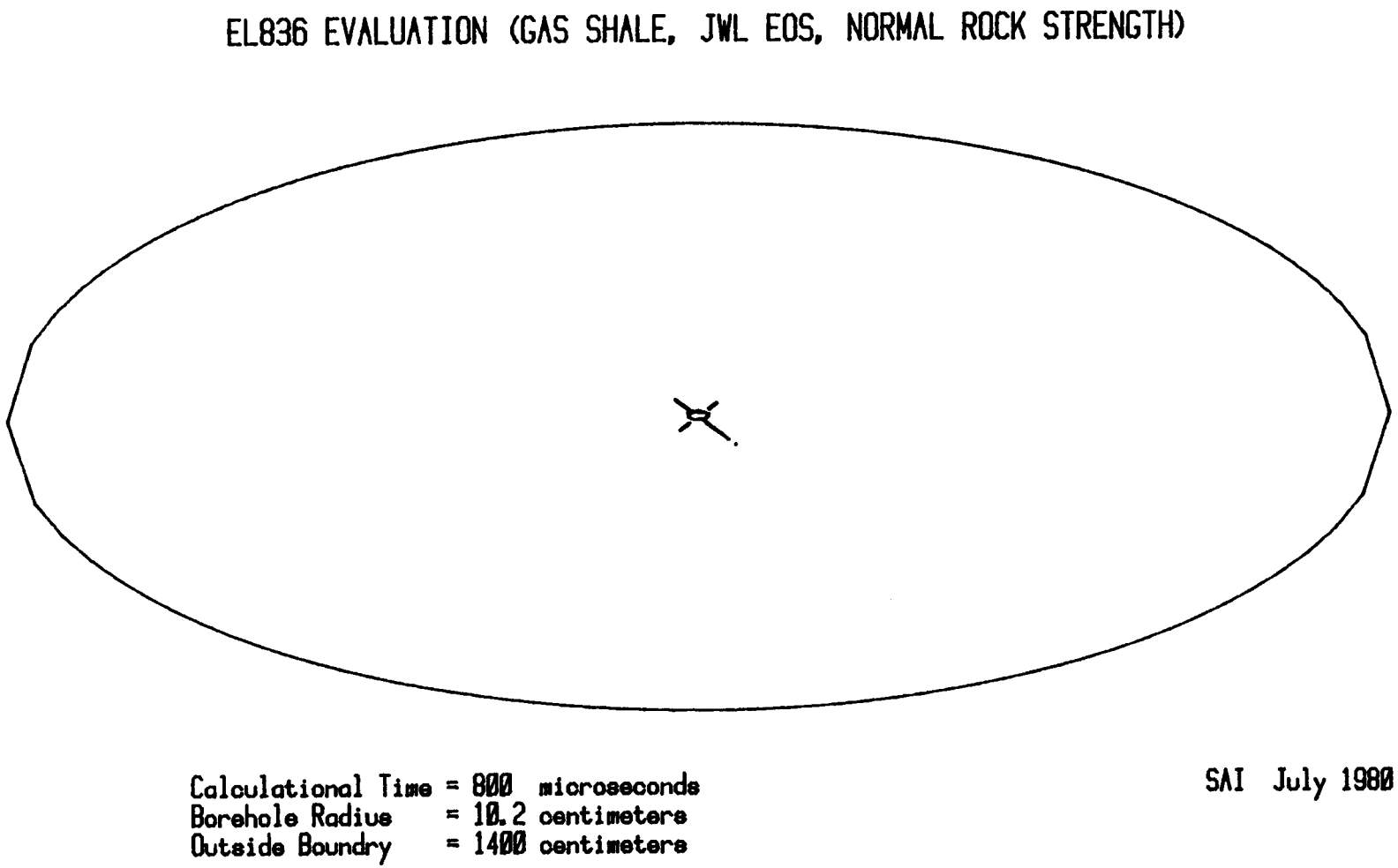

Figure 15. EL836 Stimulation of Gas Shale

EL836 EVALUATION (GAS SHALE, JWL EOS, NORMAL ROCK STRENGTH)

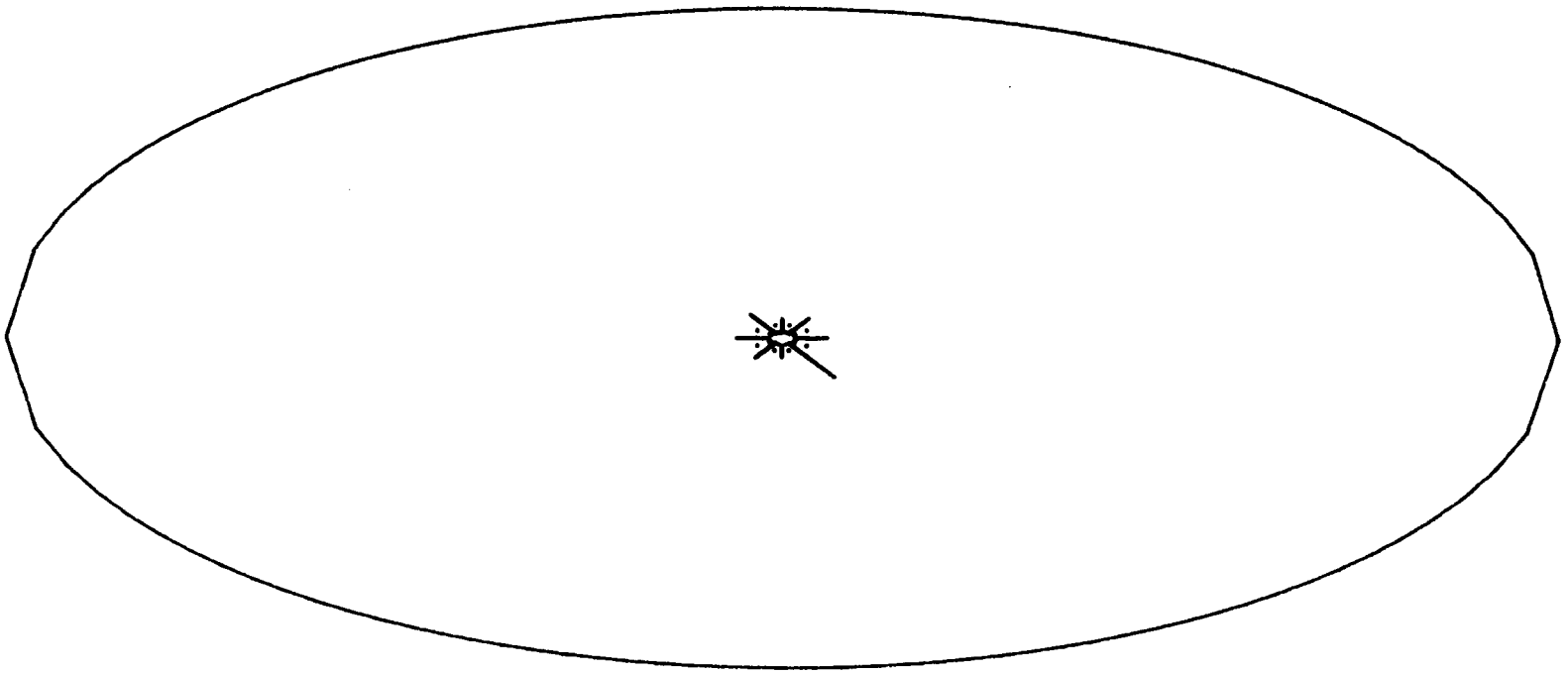

Calculational Time = 900 microseconds
Borehole Radius = 10.2 centimeters
Outside Boundry = 1400 centimeters

SAI July 1980

Figure 16. EL836 Stimulation of Gas Shale

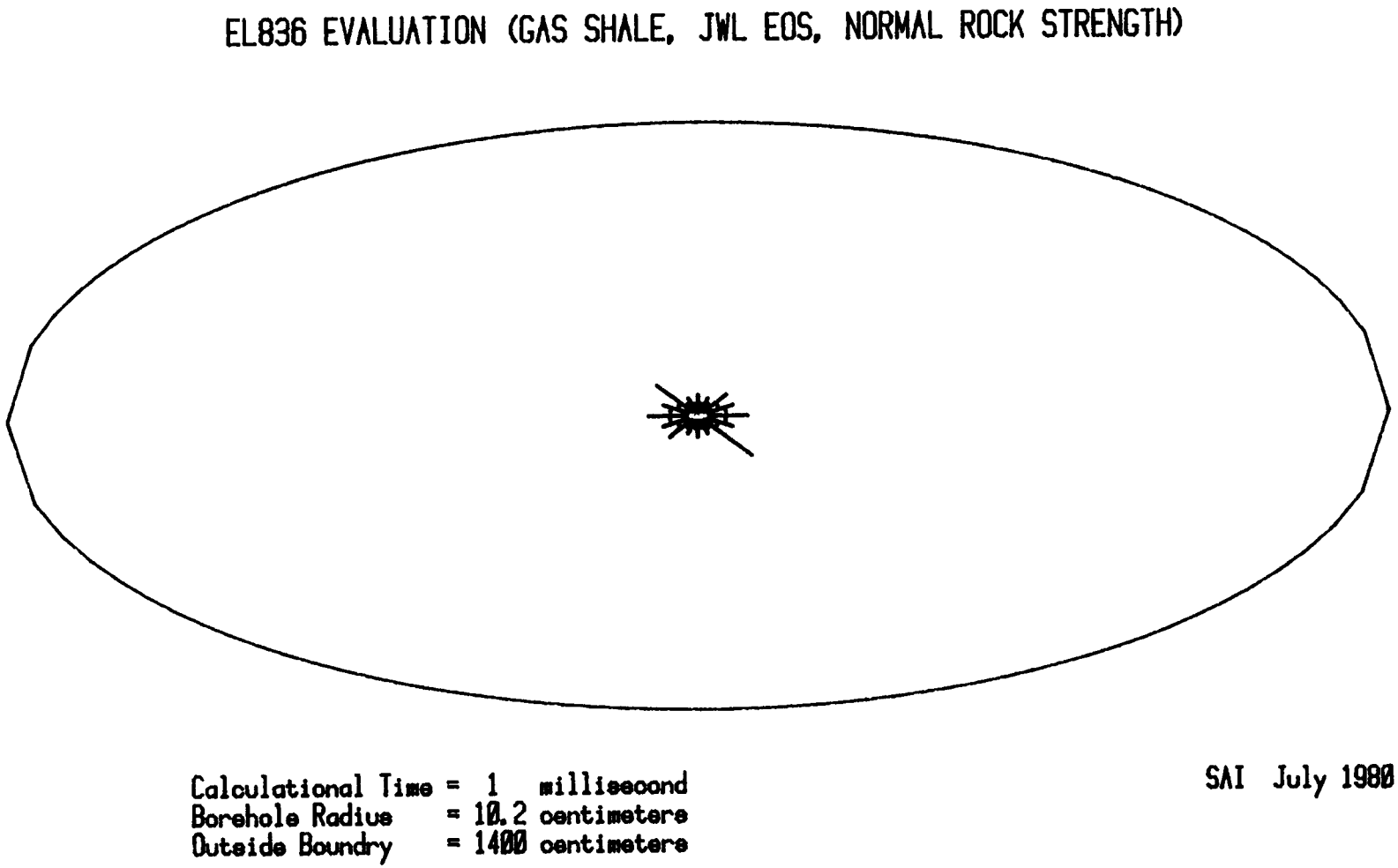

Figure 17. EL836 Stimulation of Gas Shale

EL836 EVALUATION (GAS SHALE, JWL EOS, NORMAL ROCK STRENGTH)

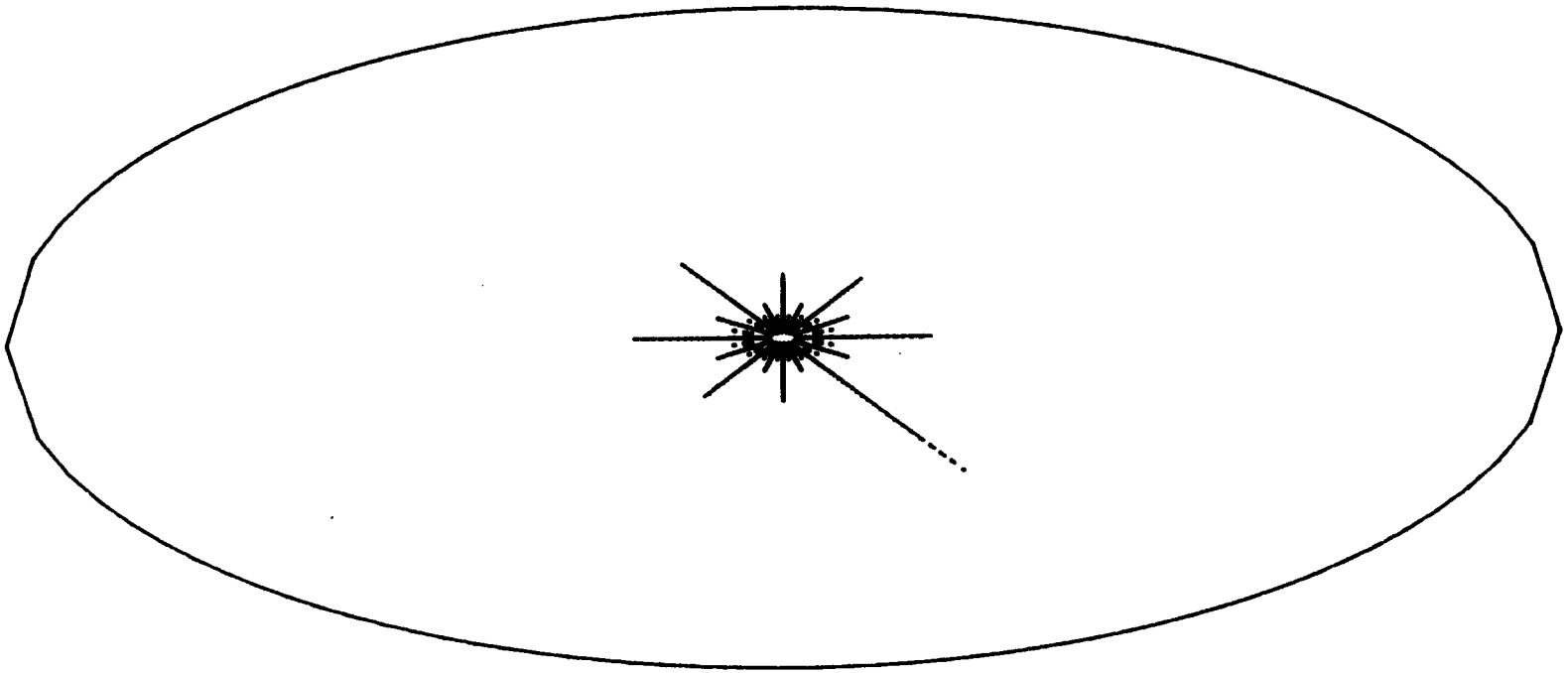

Calculational Time = 2 milliseconds
Borehole Radius = 10.2 centimeters
Outside Boundry = 1400 centimeters

SAI July 1980

Figure 18. EL836 Stimulation of Gas Shale

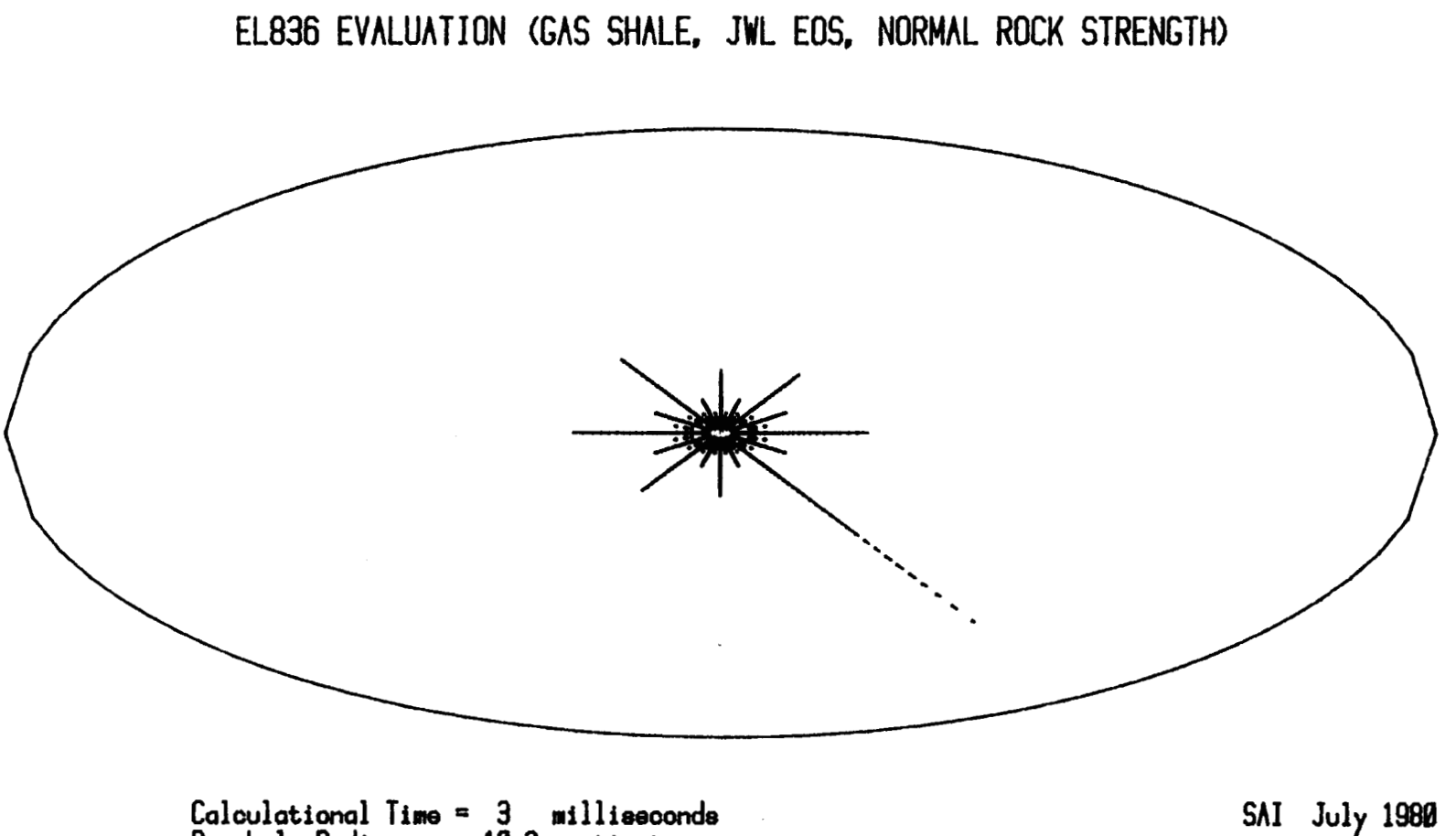

Figure 19. EL836 Stimulation of Gas Shale

EL836 EVALUATION (GAS SHALE, DUPONT EOS, NORMAL ROCK STRENGTH)

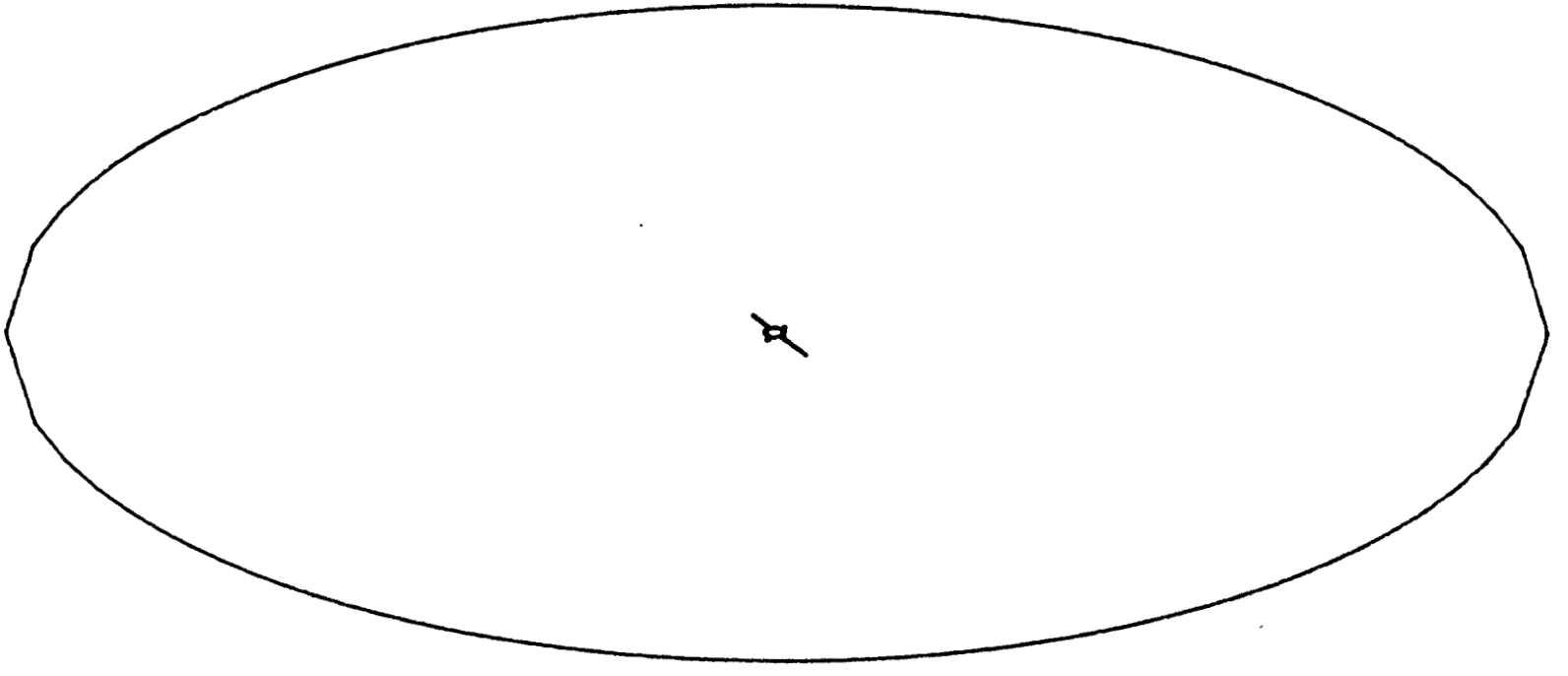

Calculational Time = 800 microseconds
Borehole Radius = 10.2 centimeters
Outside Boundry = 1400 centimeters

SAI July 1980

Figure 20. EL836 Stimulation of Gas Shale

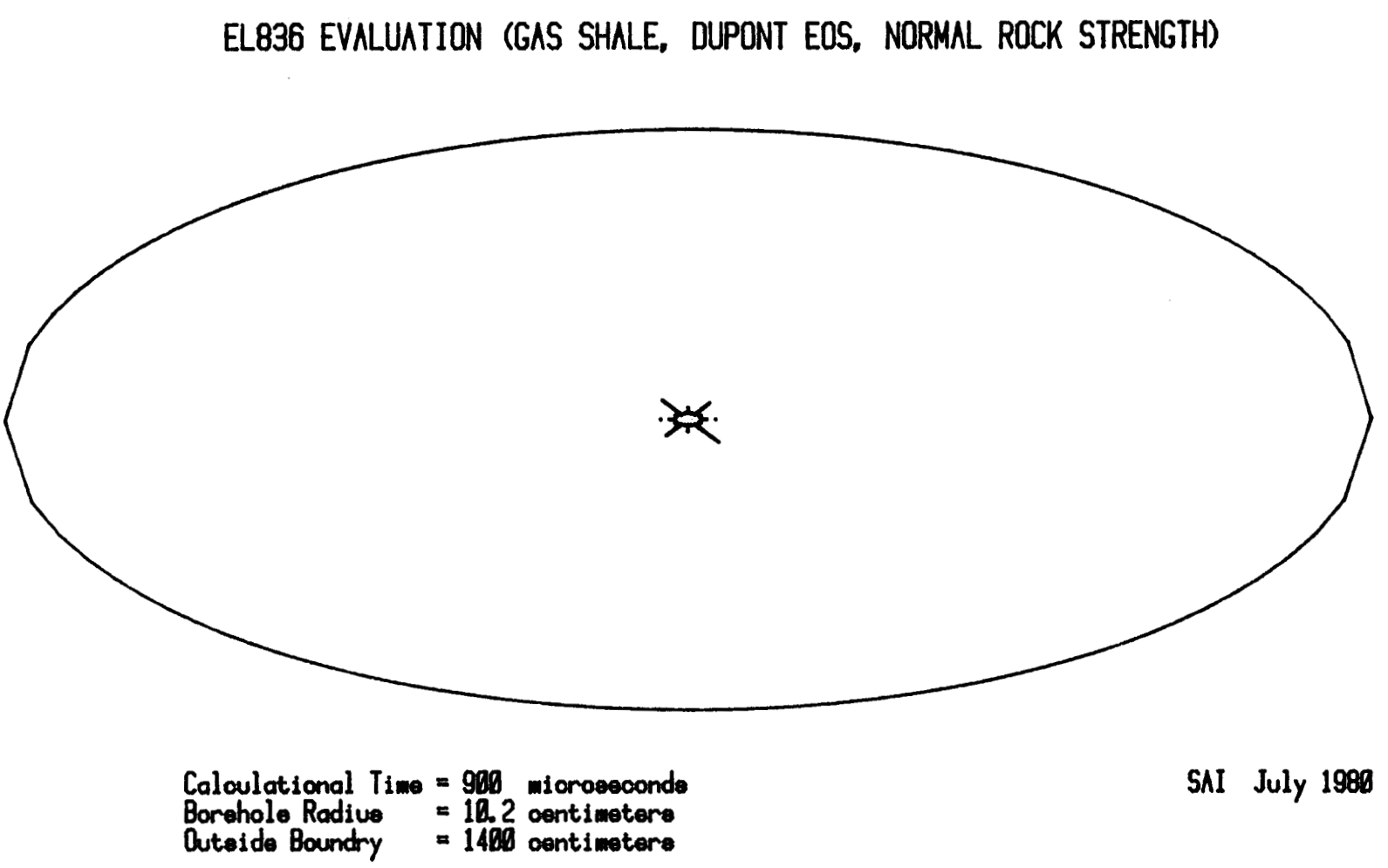

Figure 21. EL836 Stimulation of Gas Shale

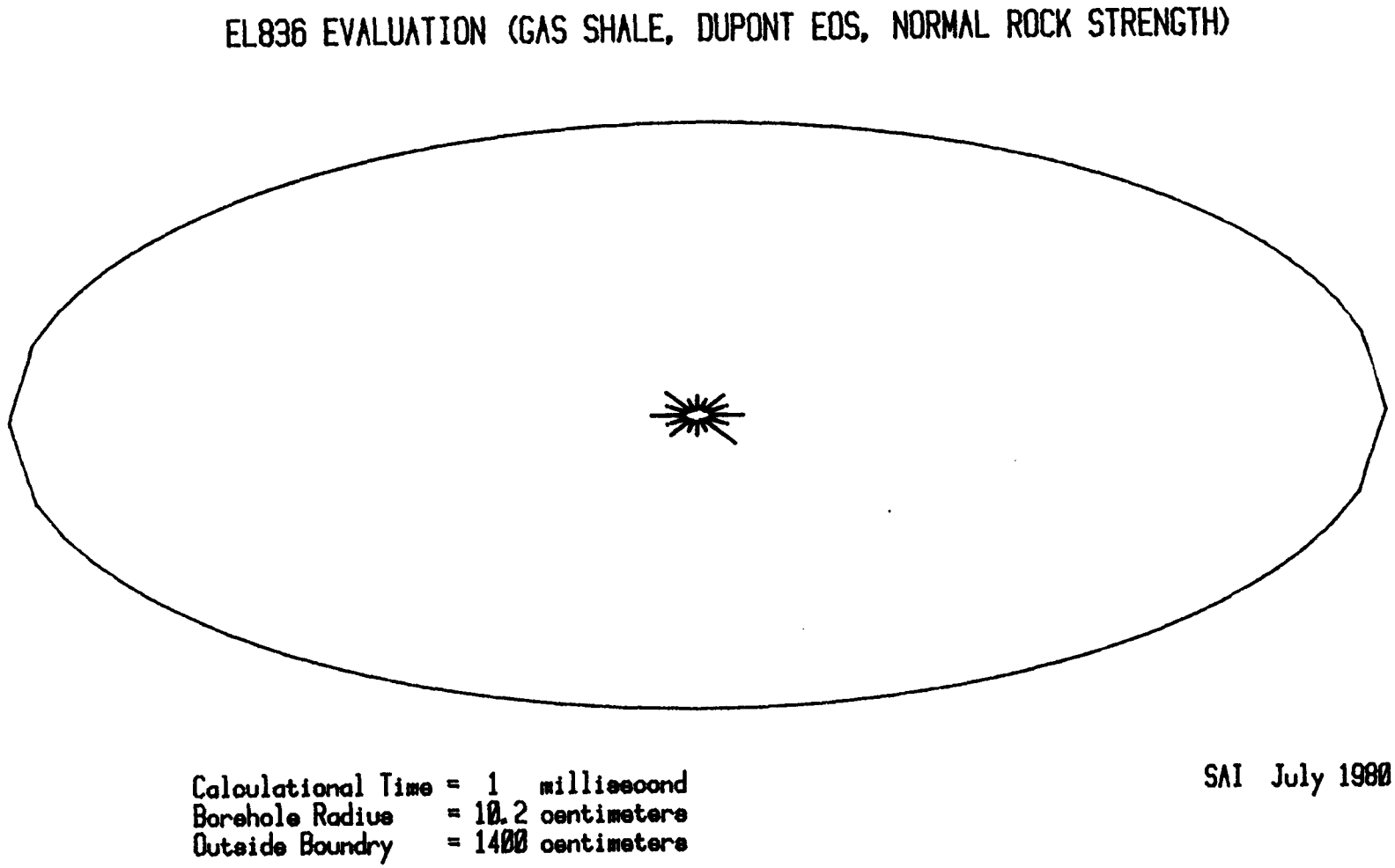

Figure 22. EL836 Stimulation of Gas Shale

EL836 EVALUATION (GAS SHALE, DUPONT EOS, NORMAL ROCK STRENGTH)

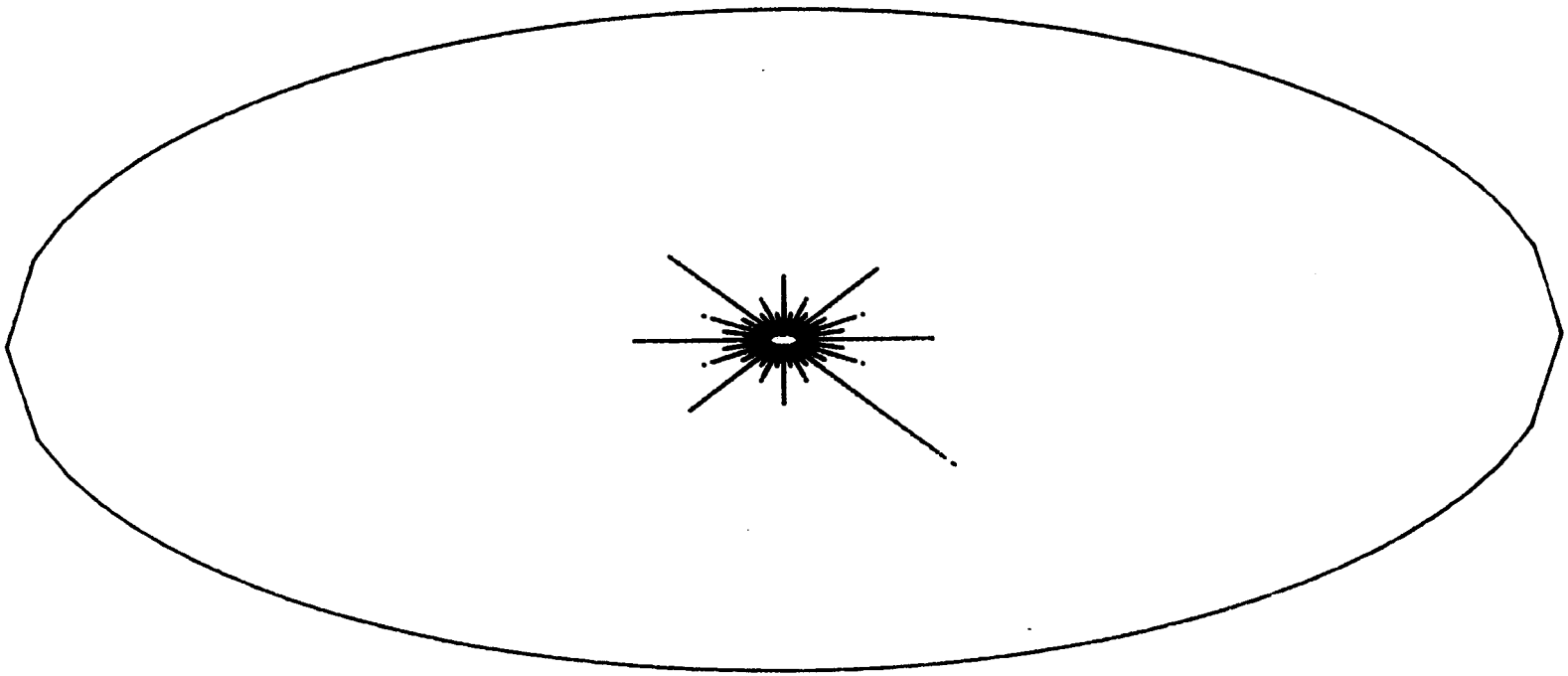

Calculational Time = 2 milliseconds
Borehole Radius = 10.2 centimeters
Outside Boundry = 1400 centimeters

SAI July 1980

Figure 23. EL836 Stimulation of Gas Shale

EL836 EVALUATION (GAS SHALE, DUPONT EOS, NORMAL ROCK STRENGTH)

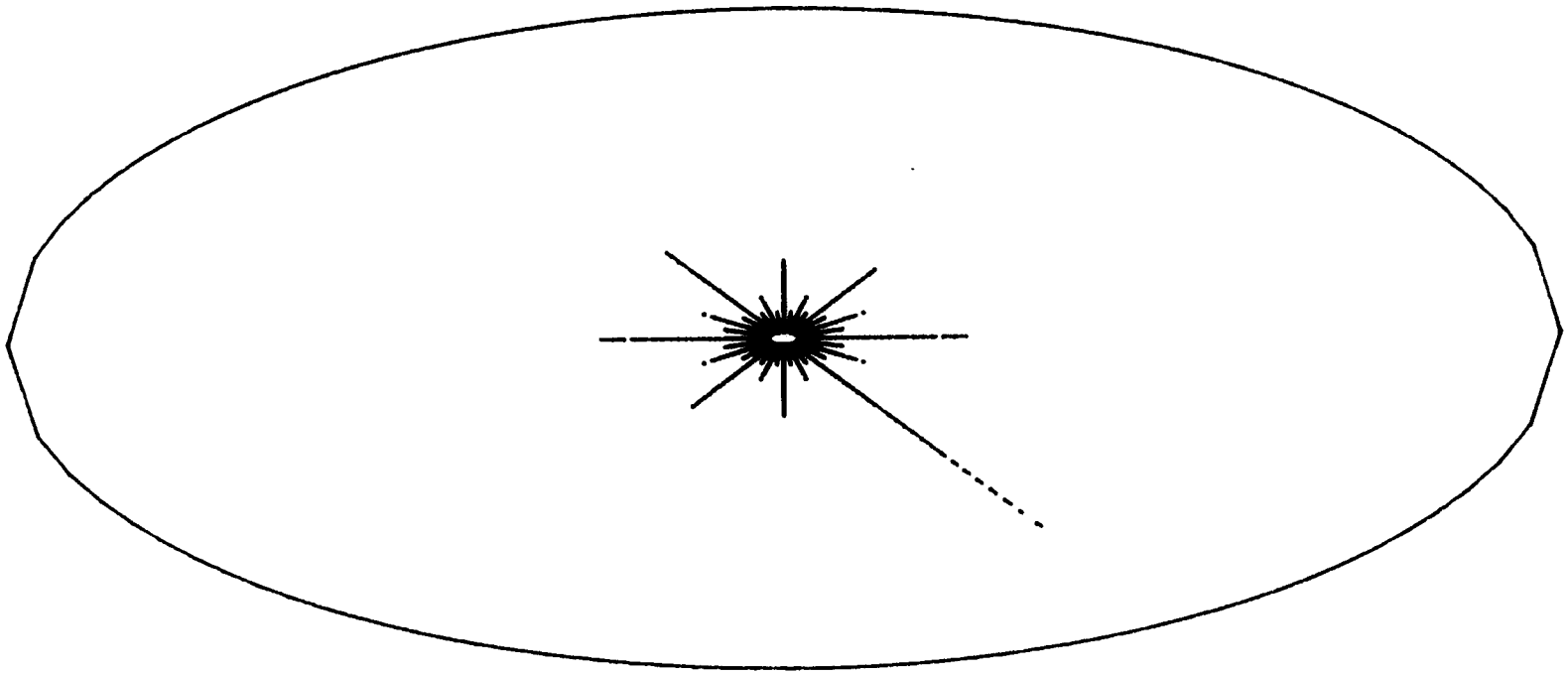

Caloulational Time = 3 milliseconds
Borehole Radius = 10.2 centimeters
Outside Boundry = 1400 centimeters

SAI July 1980

Figure 24. EL836 Stimulation of Gas Shale

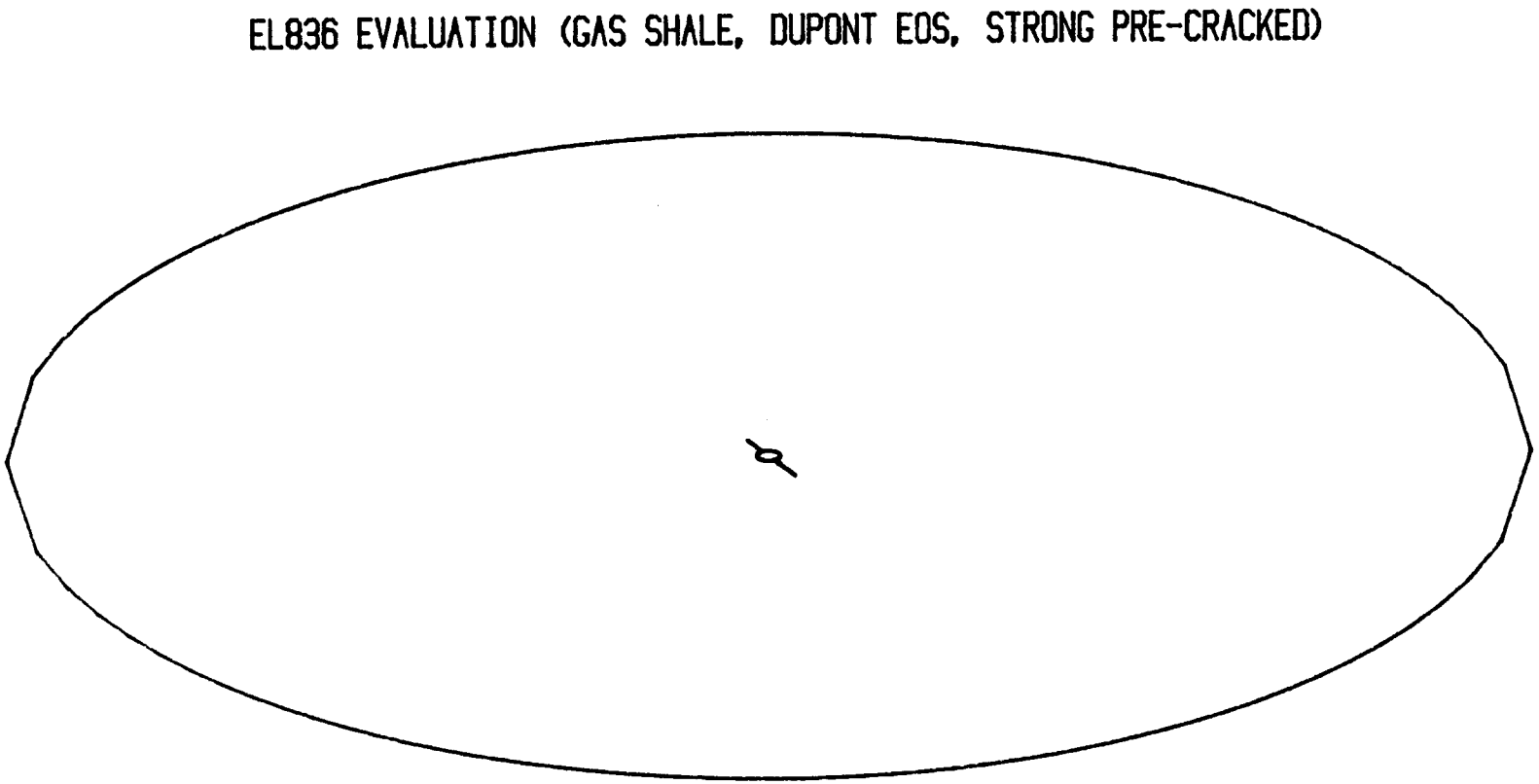

Figure 25. EL836 Stimulation of Gas Shale

EL836 EVALUATION (GAS SHALE, DUPONT EOS, STRONG PRE-CRACKED)

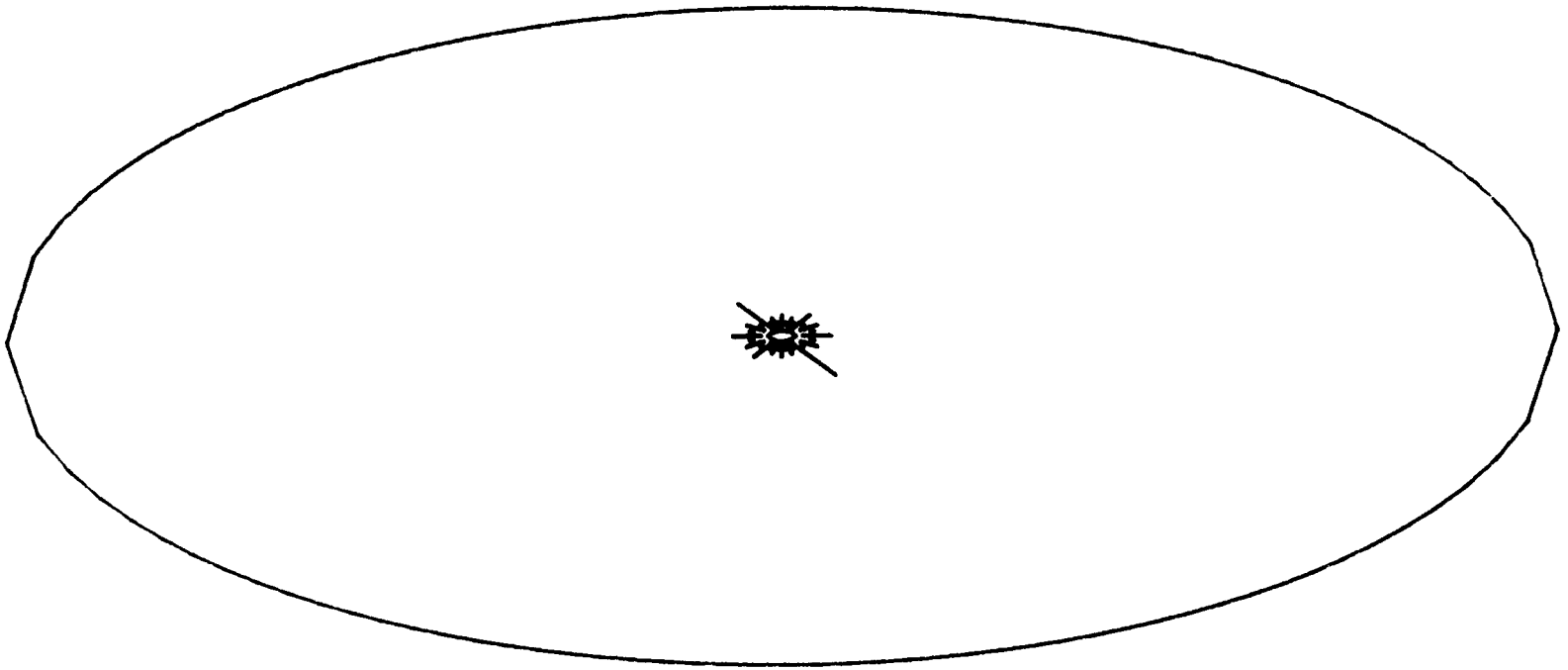

Calculational Time = 800 microseconds
Borehole Radius = 10.2 centimeters
Outside Boundry = 1400 centimeters

SAI July 1980

Figure 26. EL836 Stimulation of Gas Shale

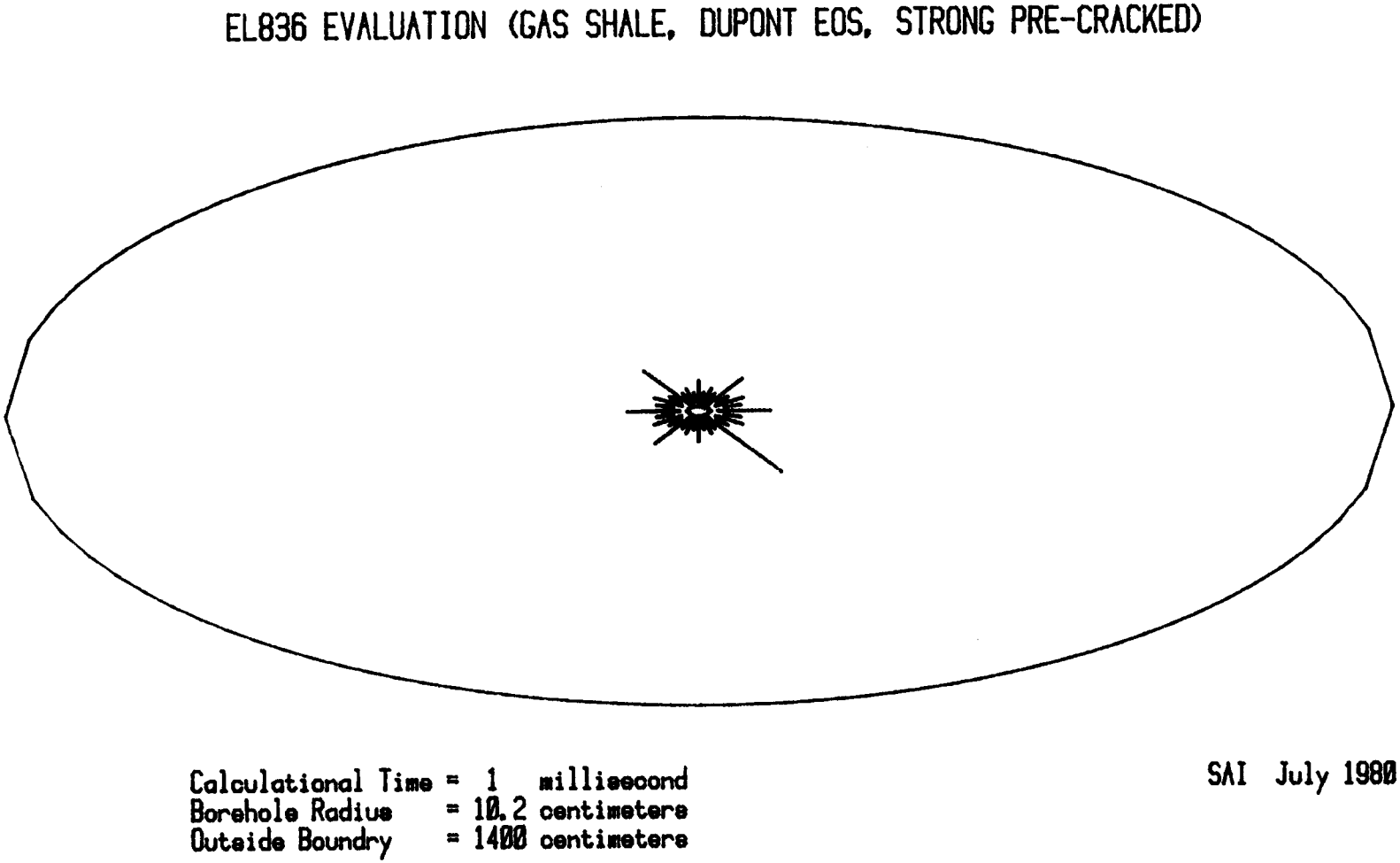

Figure 27. EL836 Stimulation of Gas Shale

EL836 EVALUATION (GAS SHALE, DUPONT EOS, STRONG PRE-CRACKED)

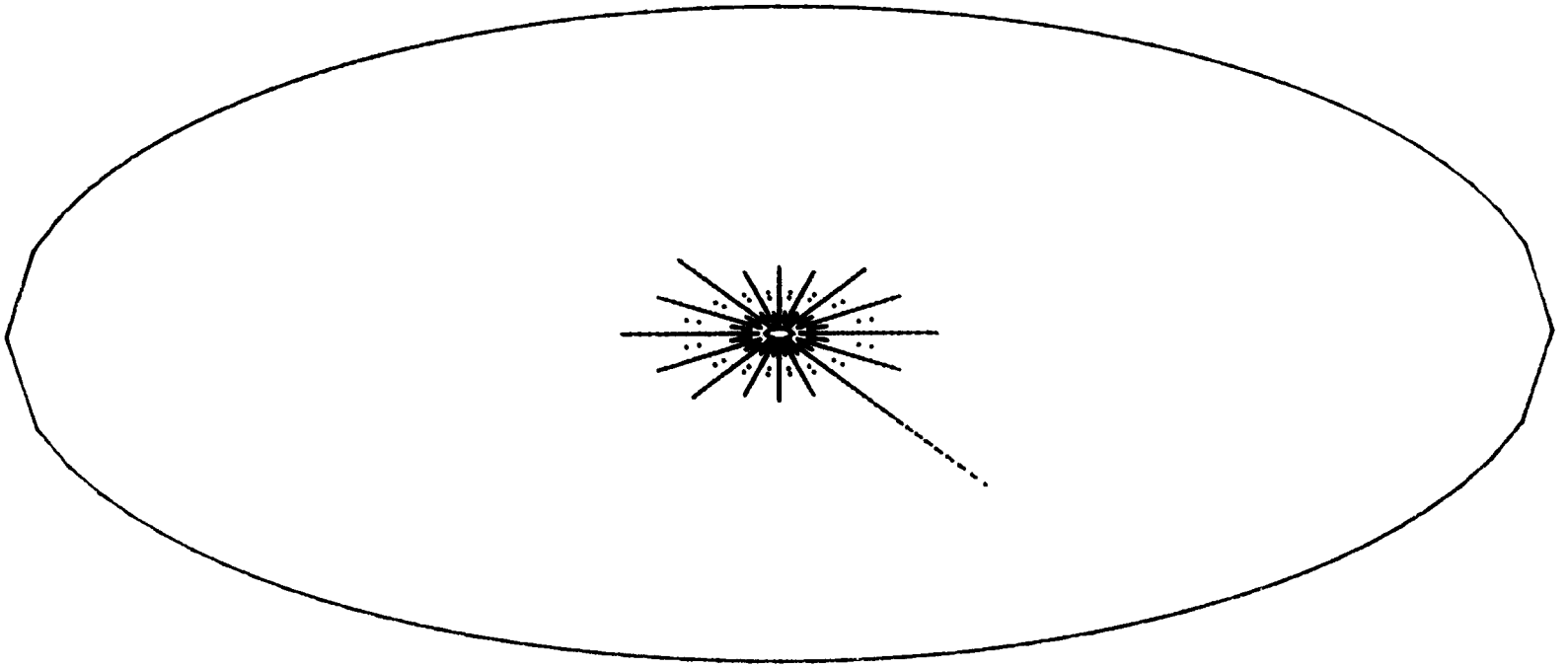

Calculational Time = 2 milliseconds
Borehole Radius = 10.2 centimeters
Outside Boundry = 1400 centimeters

SAI July 1980

Figure 28. EL836 Stimulation of Gas Shale

EL836 EVALUATION (GAS SHALE, DUPONT EOS, STRONG PRE-CRACKED)

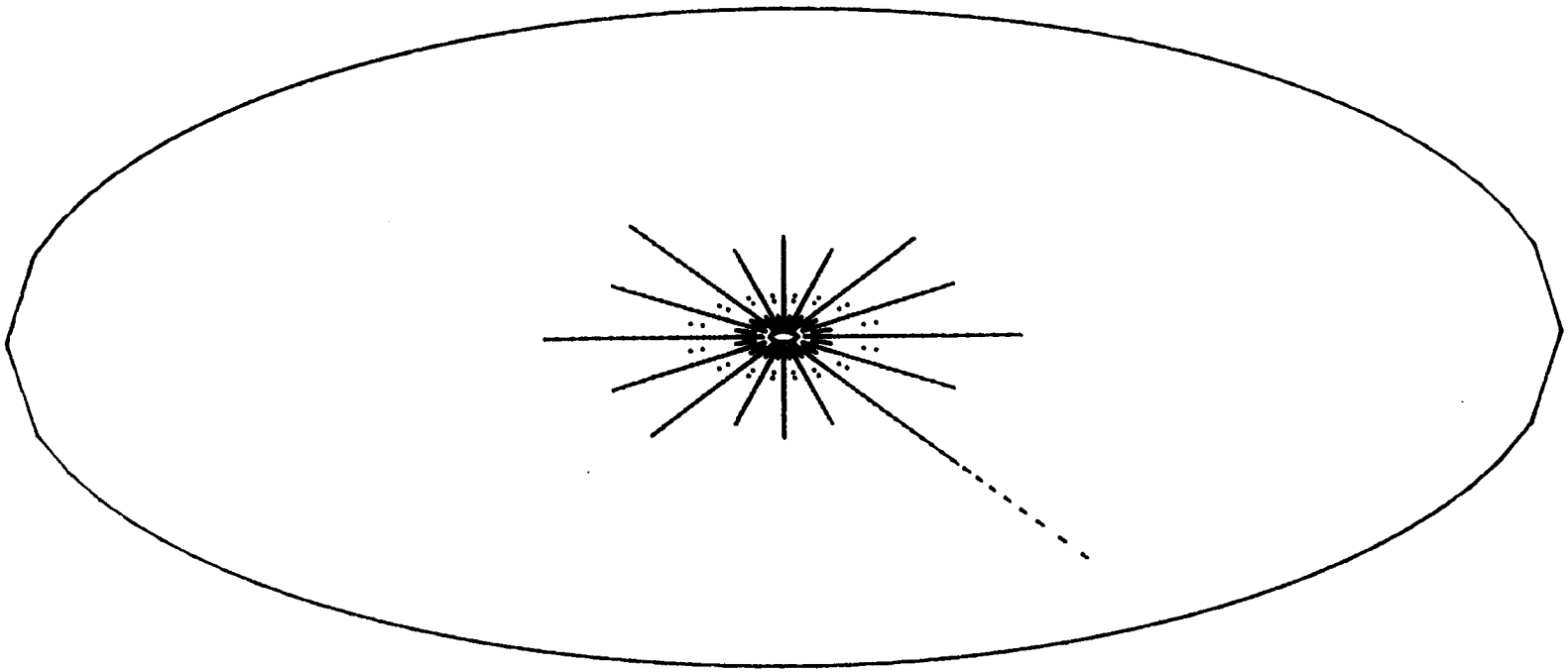

Calculational Time = 3 milliseconds
Borehole Radius = 10.2 centimeters
Outside Boundry = 1400 centimeters

SAI July 1980

Figure 29. EL836 Stimulation of Gas Shale

EL836 EVALUATION (GAS SHALE, DUPONT EOS, STRONG PRE-CRACKED)

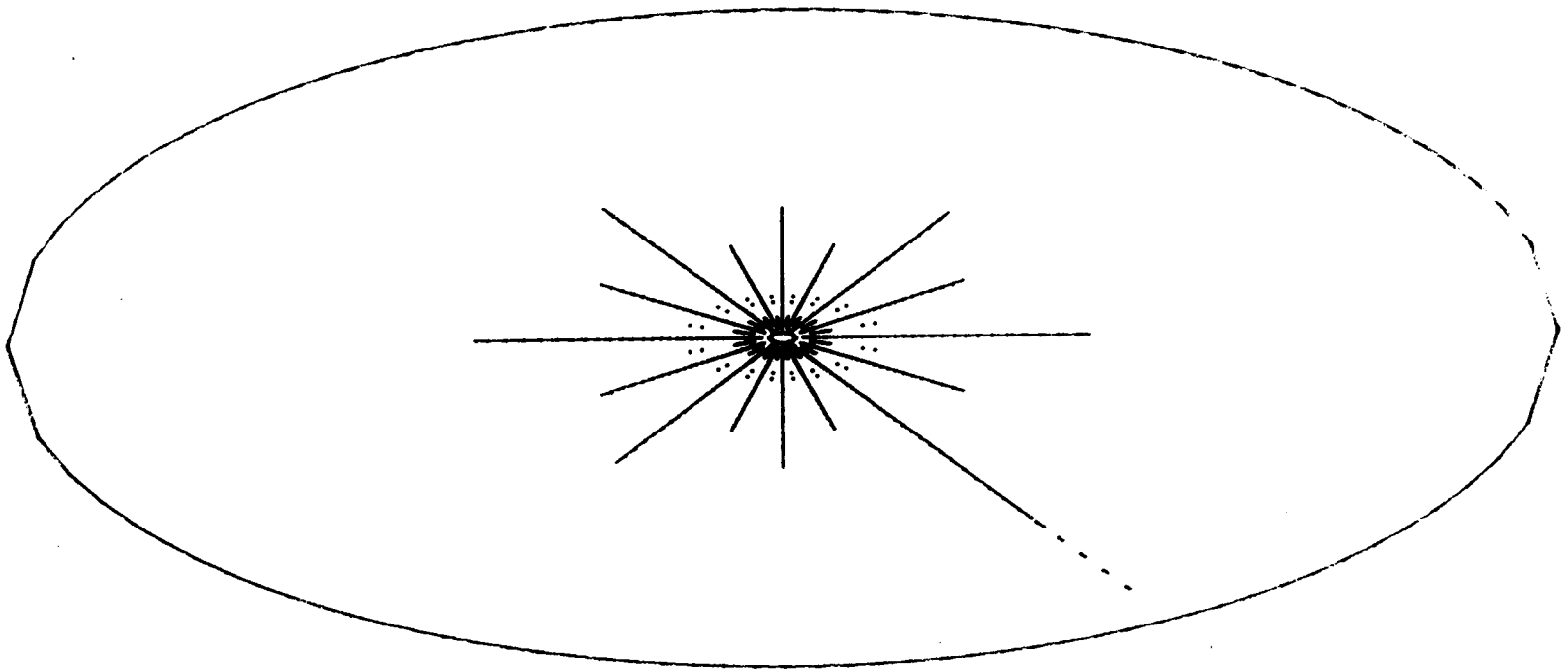

Calculational Time = 4 milliseconds
Borehole Radius = 10.2 centimeters
Outside Boundry = 1400 centimeters

SAI July 1980

Figure 30. EL836 Stimulation of Gas Shale

EL836 EVALUATION (GAS SHALE, DUPONT EOS, STRONG PRE-CRACKED)

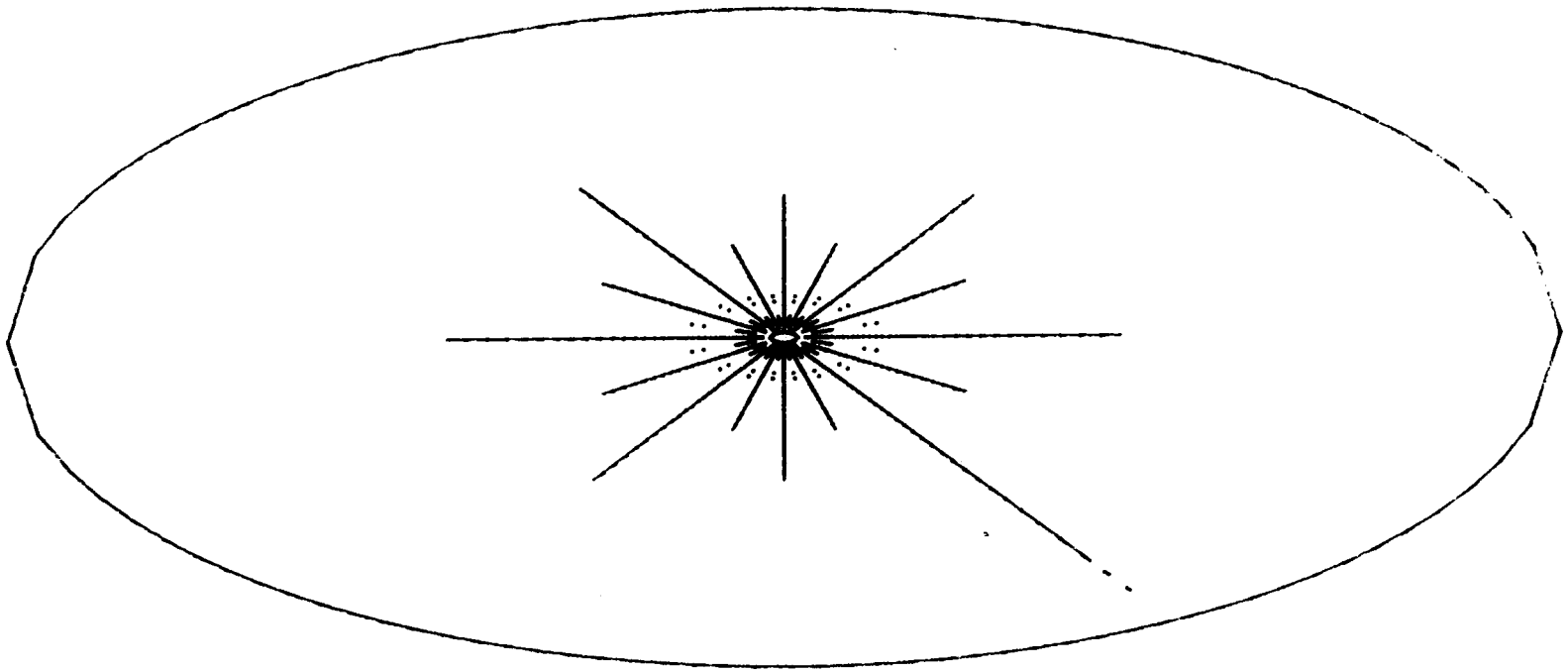

Calculational Time = 5 milliseconds
Borehole Radius = 10.2 centimeters
Outside Boundry = 1400 centimeters

SAI July 1980

Figure 31. EL836 Stimulation of Gas Shale

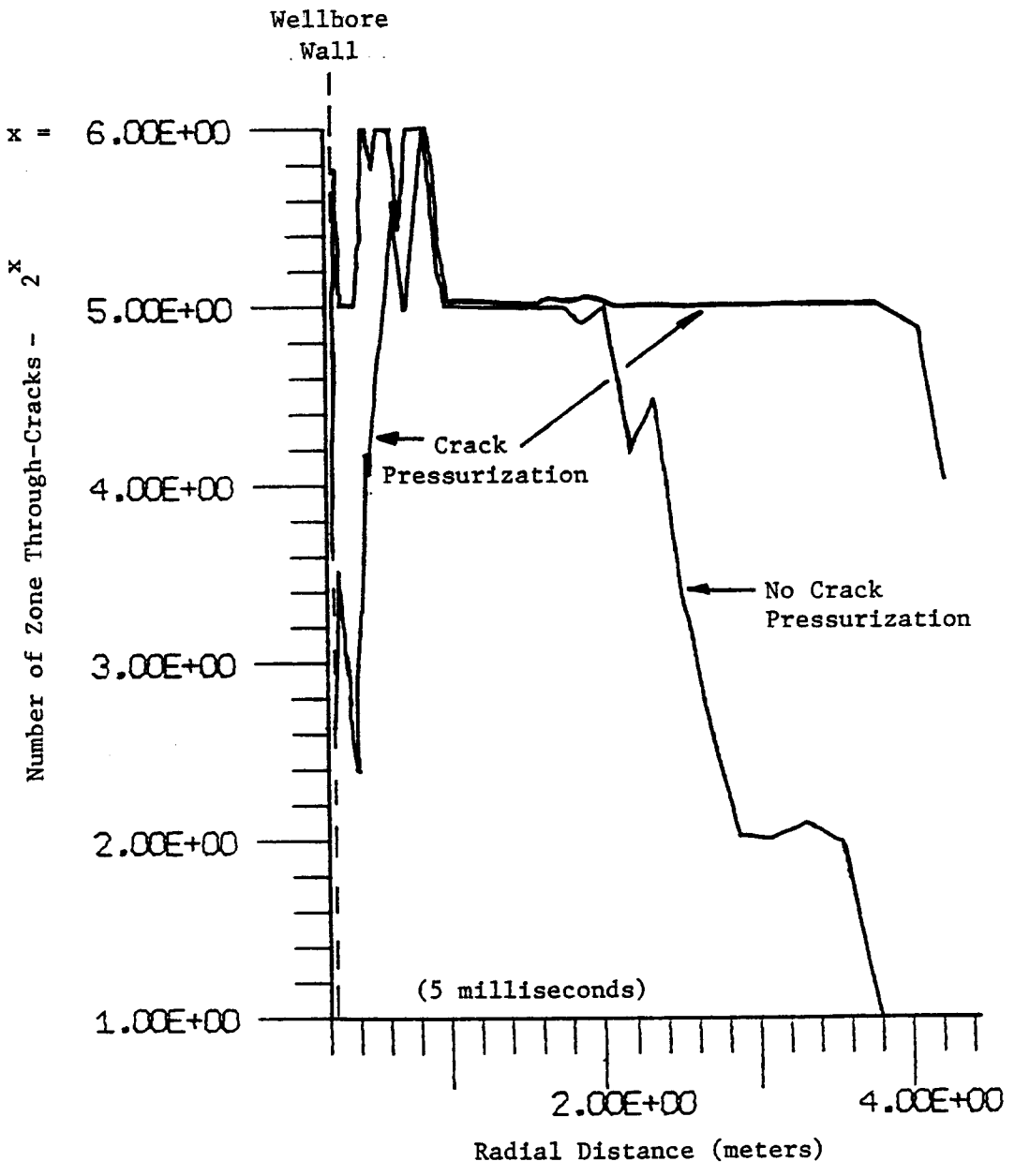

Figure 32. EL836 Stimulation - Number of Cracks vs Radial Distance, Crack Pressurization and No Crack Pressurization.

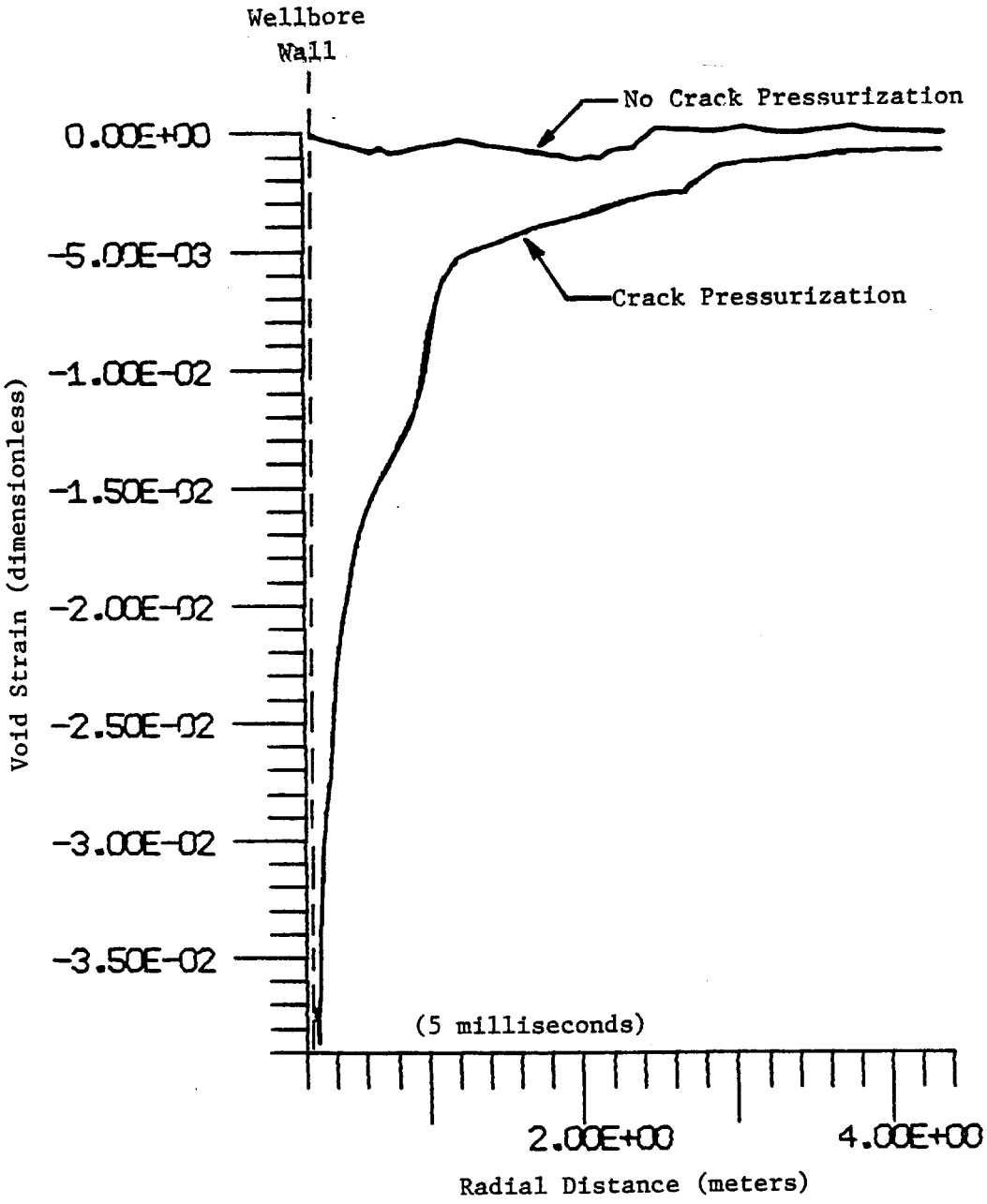

Figure 33. EL836 Stimulation - Void Strain vs Radial Distance, Crack Pressurization and No Crack Pressurization